ENGINEERING ANALYSIS OF FUGITIVE PARTICULATE MATTER EMISSIONS FROM CATTLE FEEDYARDS

A Thesis

by

LEE BRADFORD HAMM

Submitted to the Office of Graduate Studies of
Texas A&M University
in partial fulfillment of the requirements for the degree of

MASTER OF SCIENCE

December 2005

Major Subject: Biological and Agricultural Engineering

ENGINEERING ANALYSIS OF FUGITIVE PARTICULATE MATTER EMISSIONS FROM CATTLE FEEDYARDS

A Thesis

by

LEE BRADFORD HAMM

Submitted to the Office of Graduate Studies of
Texas A&M University
in partial fulfillment of the requirements for the degree of

MASTER OF SCIENCE

Approved by:

Chair of Committee,	Calvin B. Parnell, Jr.
Committee Members,	Ronald Lacewell
	Bryan W. Shaw
Head of Department,	Gerald Riskowski

December 2005

Major Subject: Biological and Agricultural Engineering

ABSTRACT

Engineering Analysis of Fugitive Particulate Matter Emissions from Cattle Feedyards.

(December 2005)

Lee Bradford Hamm,

B.S., Texas A&M University

Chair of Advisory Committee: Dr. Calvin B. Parnell, Jr.

An engineering analysis of the fugitive particulate matter emissions from a feedyard is not simple. The presence of an evening dust peak in concentration measurements downwind of a feedyard complicates the calculation of an average 24-h emission flux for the feedyard. The evening dust peak is a recurring event that occurs during evening hours when particulate matter concentration measurements increase and decrease dramatically during a short period of time. The concentrations measured during the evening can be up to 8 times the concentrations measured throughout the rest of the day. There is a perception that these concentration increases are due to increases in cattle activity as the temperature decreases during the evening. The purpose of Objective 1 of this research was to quantify the changes in concentrations based on changes in meteorological conditions and/or cattle activity. Using ISCST3, a Gaussian-based EPA-approved dispersion model used to predict concentrations downwind of the feedyard , the results of this work indicate that up to 80% of the increase in concentrations can be attributed to changes in meteorological conditions (wind speed, stability class, and mixing height.)

The total fugitive particulate matter emissions on a cattle feedyard are due to two sources: unpaved roads (vehicle traffic) and pen surfaces (cattle activity). Objective 2 of this research was to quantify the mass fraction of the concentration measurements that was due to unpaved road emissions (vehicle traffic). A recent finding by Wanjura et al. (2004) reported that as much as 80% of the concentrations measured after a rain event were due to unpaved road emissions. An engineering analysis of the potential of the unpaved road emissions versus the total feedyard emissions using ISCST3 suggests that it is possible for 70 to 80% of the concentration measurements to be attributed to unpaved road emissions.

The purpose of Objective 3 was to demonstrate the science used by ISCST3 to predict concentrations downwind of an area source. Results from this study indicate that the ISCST3 model utilizes a form of the Gaussian line source algorithm to predict concentrations downwind of an area source.

ACKNOWLEDGMENTS

I would like to personally thank the members of my advisory committee, as they provided me with an opportunity to further my education, especially Dr. Parnell, who believed in me even when I didn't. I would like to thank my committee for their insight and knowledge, especially for getting me out of binds that I wouldn't have been able to get out of myself. I would also like to thank Dr. Shaw for his mentoring, especially for helping me out when I most needed it.

I would like to thank each of the Crew members for the time that I spent during graduate school. You all have become good friends who go to great lengths to help someone out, especially one of your own. Barry thank you for the hard but funny times that you gave me. John, nobody ever recognizes you for all of the hard work that you do, so here's to you. Thanks for being a great friend and gathering information that could be used by many people. Brock, even though you and I knew each other in the band, I only really got to know you once we started working together. With your dedication and helping hand, I know you will go far. Jackie, even though Barry and I messed with you the entire time you were in grad school, I am glad that things are turning out so well for you and hope that they continue to do so. To Tree, Stump, Na-dam-thaniel, Marky Mark, Bonz, and Stanley, thanks for being great student workers, and helping me to realize that life should be more about laughing than working. To Cale and Ordway, I know nobody tells you this, but the two of you make great friends and have made me appreciate both of you over the past two years.

I would especially like to thank my family. My parents, Jim and Donna, deserve great thanks for helping me through my undergrad years, especially my fish year and the following years in the Corps. They also continued to support me through grad school, even when I was going through some tough times. I would also like to thank my brother, Reed, for making my life the blast that it was growing up, and the continued harassment that we wreak upon each other. I would also like to thank my mother- and father-in–law, Charles and Sharon, who only really got to know me after I started graduate school, and still liked me anyway.

My greatest thanks belong to my wife, Sarah, who married me even though we had to put our life on hold for me to go to graduate school. Your support, laughter, and love were some of the only things that kept me going in my darker times. May I prove to be as good to you as you were to me.

And last I would like to thank the Lord, our God; who, though we may not believe in Him; He always believes in us.

TABLE OF CONTENTS

Page

TABLE OF CONTENTS (Continued)

Page

LIST OF FIGURES

Page

LIST OF TABLES

Page

INTRODUCTION

The introduction of the Clean Air Act (CAA) in 1963 was an attempt by the federal government to address growing environmental concerns in the United States. The Reorganization Plan No. 3 of 1970 created the Environmental Protection Agency (EPA), and the Clean Air Act amendments of 1970 provided power and responsibilities to the EPA to develop and enforce regulations for the protection of the general public (CAA, 1990). Further amendments to the Clean Air Act passed by Congress in 1977 and 1990 expanded EPA's authority over various aspects of air pollution regulation (CAA, 1990).

EPA is the federal agency responsible for the oversight of all rules and regulations, permitting, and enforcement programs used by State Air Pollution Regulatory Agencies (SAPRA). Each SAPRA is required by the EPA to submit a State Implementation Plan (SIP) that details the programs a SAPRA will utilize to carry out its responsibilities as described in the CAA. SIPs are compilations of the policies and regulations used by a SAPRA to promote air quality. The CAA requires the EPA to approve each SIP. If a SIP is unacceptable, the EPA has authority under the CAA to assume control of federal operating permit program in that state (CFR, 1996).

There are permitting programs designed to aid in preventing pollution, controlling pollution that already exists, and funding the SAPRA. The federal permitting programs can be placed into two categories: New Source Review (NSR) (CFR, 1986b) and operating (PSD and Title V). The main federal pre-construction permits are the New Source Review (NSR) permits (CFR, 1986b).

This thesis follows the style of *Transactions of the ASAE.*

The Title V permit program may be delegated by the EPA to the SAPRA for implementation (CFR, 1996). To be required to obtain Title V and Prevention of Significant Deterioration (PSD) permits, an emission source must emit or have the potential to emit regulated pollutants above certain thresholds. These thresholds are dependent upon the pollutant and whether or not the area around the source is in an attainment area. An attainment area is defined as *a geographic area in which levels of a criteria air pollutant meet the health-based primary standard (NAAQS) for the pollutant.* (CAA, 1990) The National Ambient Air Quality Standards (NAAQS) (CFR, 1999) are health-based concentration limits above which ambient concentration measurements are deemed an "exceedance". In addition, some states use the NAAQS as concentrations at the property line of the emission source that are not to be exceeded. An inaccurate emission factor used by a SAPRA with dispersion modeling to predict property line concentrations would result in incorrect predicted concentrations. Repercussions could include inappropriate regulation of sources if exceedances of the NAAQS are detected based on inaccurate concentration estimates from modeling or measurements.

All facilities with sources of criteria pollutants are required to obtain NSR permits before construction can begin (CFR, 1986a). NSR permits include allowable emission rates of pollutants for each source. The annual emissions from these facilities are referred to as emissions inventories (EI) and are reported in mass of pollutants per year (CFR, 1986a). EI may consist of annual emissions of all pollutants emitted including stationary and fugitive sources.

For cattle feedyards, fugitive particulate matter (PM) emissions include the PM emissions from the feedyard pen surface as a consequence of cattle activity and the

unpaved roads as a consequence of vehicle traffic. PM emission factors have been developed by the EPA and EPA contractors to aid SAPRA to estimate the EI based on cattle populations. The resulting fugitive EI are the total emissions that can be expected from the feedlot surface. The EPA has also developed a PM emission factor for the unpaved road emissions. Both of these PM emission factors appeared at one time in the AP-42 (USEPA, 1995) document in which the EPA published its emission factors. Currently, the cattle feedyard emission factor has been removed from the fifth edition of the AP-42 document.

The data used to develop the PM emission factor in AP-42 for cattle feedyards were the results of a study that occurred in the early 1970's when the California Cattle Feeders Association (CCFA) (Algeo et al., 1972) wanted to acquire information about the dust that was emanating from the feedyards and the possible impacts that it had on their operations. The information gathered by this study was presented in four bulletins published by the CCFA. (Algeo et al., 1972) The data included PM concentrations from 25 feedyards with measurements taken on a 24-hour basis.

The data gathered by the CCFA study were used by Peters and Blackwood (1977) for the development of a cattle feedyard total suspended particulate (TSP) fugitive emission factor for the USEPA. Peters and Blackwood (1977) reported an emission factor for TSP of 127 kg/ 1000 hd-day (280#/1000hd-day) for the feedyard surface and their emission factor was included in AP-42 (USEPA, 1985). Parnell et al. (1999) reported errors in the process used by Peters and Blackwood (1977) to develop the TSP AP-42 emission factor. These errors include:

- assuming the emission height for the cattle was ten feet;

- no measured meteorological data, so the national average of 4.47 m/s was used along with a stability class of C (which doesn't occur at night);
- assuming 8000 head of cattle when the numbers for the feedyards were not reported in Algeo's study;
- assuming that all yards were square.

Sweeten et al. (1988, 1998) performed ambient sampling on cattle feedyards to determine the ratio between TSP and PM_{10}. The results of this research were that the fraction of TSP that is PM_{10} was approximately twenty-five percent for cattle feedyard dust. This study, combined with the emission factor that Peters and Blackwood developed, resulted in a PM_{10} emission factor of 31.8 kg/1000 hd-day (70 lb/1000 hd-day). Parnell et al. (1993), using the data gathered by Sweeten throughout 1987, reported a more appropriate emission factor for PM_{10} of 4.54 kg/1000hd-day (10#/1000 hd-day). This was determined by using the Fugitive Dust Model and calculating the area fluxes based on the measured concentrations. The emissions were shown to vary with the time of year, with the highest occurring in April and the lowest in January (Parnell et al., 1993). The reported emission factors were an average of 4.2 kg/1000 hd-day (9.2 lb/1000 hd-day) and the seasonally weighted factor 4.6 kg/1000 hd-day (10.2 lb/1000hd-day).

Parnell et al. (1999) reported results of a study funded by the Texas Natural Resources Conservation Commission (TNRCC) that included multiple sampling tests at cattle feedyards. The results of this study was a recommendation that the emission factor of 6.8 kg/1000hd-day (15 lb/1000 hd-day) be used to calculate annual fugitive PM emissions from cattle feedyards.

Cattle feedyards may be required to reduce their fugitive PM emissions by SAPRAs at any time. If a cattle feedlot is located in a non-attainment area for PM_{10}, it is likely that the SAPRA will require reduction of its fugitive PM emissions. The magnitude of the required reduction will be based upon the emission factors used. If the PM emission factors for fugitive emissions from cattle feedyards are incorrect, penalties may be applied against feedyards inappropriately. It is also necessary to discern from where the emissions originate, i.e. the unpaved roads or the feedlot surface. When the sources of fugitive emissions for a cattle feedyard and how much they contribute to concentration measurements are determined, measures for reducing these emissions can be used more efficiently and effectively.

The goal of this research was to accumulate information for the development of accurate emission factors for fugitive PM_{10} emissions from a cattle feedyard. The protocol for obtaining science-based PM emission factors has been improved (Wanjura et al., 2004). Meteorological conditions play a large role in the process of back-calculating emission rates from measured ambient concentrations as does the sources of the particulate matter emissions.

During sampling trips to cattle feedyards (Sweeten et al., 1988; Parnell et al., 1993; Auvermann, 2001) a phenomenon known as the evening dust peak has been observed. The evening dust peak is a repeating event on a cattle feedyard that occurs after sunset. The particulate matter concentration measurements increase and decrease in a step-function manner, with the increases a much as eight times the concentration measured throughout the rest of the day. There are three main hypotheses for these increases in concentration. One is that the increased concentrations in the evening are

due solely to cattle activity. This hypothesis is based on the current perception that cattle dramatically increase their activity in the evening as the temperature rapidly decreases (Mitloehner et al., 1999). The second is that the increases in concentration are the sole result of meteorological conditions. The reasoning behind this hypothesis is that changes in meteorological conditions increase the concentration even though the emission rate remains constant. The final hypothesis is that the concentration measurement increases in the evening are due to a combination of cattle activity and meteorological conditions. It is the purpose of Objective 1 to evaluate these hypotheses.

> Objective 1. Quantify changes in fugitive particulate matter concentrations downwind of the feedyard based on meteorological conditions and/or cattle activity.

Wanjura et al. (2004) reported that an average of over 80% of the PM emissions measured on the cattle feedyard during a sampling trip taken in April of 2004 were due to unpaved roads. The emission factor reported for the unpaved roads was 16 kg/ 1000hd-day (36 lbs/1000 hd-day). Based on this finding, unpaved roads could be a significant portion of the fugitive dust concentrations measured downwind of a feedyard. It is the purpose of Objective 2 to determine the contributions the road dust (vehicle traffic) and pen dust sources (cattle activity) of fugitive PM emissions from cattle feedyards so that effective mitigation efforts can be applied appropriately.

> Objective 2. Quantify the mass contribution of PM emissions of road dust (vehicle traffic) and pen dust (cattle activity) to the measured concentrations and ultimately PM emission rates of cattle feedyard fugitive sources.

ISCST3 performed a pivotal role in determining the results of this research. Therefore, it is important to understand the process ISCST3 utilizes to calculate concentrations downwind of an area source. The ISCST3 manual (Trinity, 2000) states

that an area source is approximated by dividing the area source into a series of line sources and using a line source algorithm to estimate the concentration downwind. Further details are unclear as to the specific mechanics involved. Work by Hamm et al. (2005) suggests that it is possible to estimate an area source using the infinite line source algorithm (ILSA). Using this method, the concentration produced downwind of a feedyard will be estimated with both ISCST3 and the ILSA. It is the purpose of Objective 3 to understand the method ISCST3 uses when estimating emissions from area sources.

> Objective 3. Compare an estimation of concentrations from a feedyard with roads using the infinite line source algorithm with concentrations produced by ISCST3 for the same feedyard setup.

METHODS

CONCENTRATION MEASUREMENTS

Two sampling trips were performed by CAAQES personnel in July, 2003 and April, 2004. The protocol and procedures used were documented by Wanjura et al. (2003) and Wang et al. (2003). The protocol called for measuring total suspended particulate (TSP) matter and PM_{10} concentrations at sampling stations on the perimeter of the yard. The total number of TSP and PM_{10} samplers varied slightly. In general, the following is the list of equipment used:

- Eight low-volume TSP samplers; (Low-volume corresponded to a nominal flow rate of 1 m^3/h in contrast to high-volume corresponding to greater than 68 m^3/h.)
- Five PM_{10} samplers; (The PM_{10} sampler heads utilized for this study were Andersen PM_{10} pre-collector sampling inlets.) Both TSP and PM_{10} samplers used Zeflour 47 mm filters.
- Rupprecht and Patashnick Tapered Element Oscillating Microbalances (TEOM) (TEOM series 1400a, Rupprecht and Patashnick, Albany, NY) fitted with CAAQES designed TSP sampler inlet heads.
- Alumatower Company 10-meter tower with three anemometers and three low-volume TSP sampling heads set at heights of 4.4, 6.5, and 9.4 m.
- Onset Computer Corporation HOBO weather station (Onset Computer Corp., Bourne, MA) used to measure wind velocity and direction, solar radiation, rainfall intensity, relative humidity, barometric pressure, and temperature.
- Data loggers (HOBO H8 RH/Temp/2x External, Onset Computer Corp., Bourne, MA) were incorporated into all low- and high-volume samplers to record the

pressure drop (Δp) across the orifice meters. Differential pressure transducers were used to measure the Δp across the orifice.

The protocol called for relatively short sampling periods between filter changes. All sampling stations were operated on a 24-hour basis during each trip. During the July 2003 trip, test durations averaged between three and four hours. Six personnel worked in two teams of three. One crew worked from eight in the morning until eight in the evening and the second crew worked the remaining 12-hour shift. During the April 2004 trip, five personnel conducted three- to four- hour sampling tests from approximately 9:00 AM until midnight. Only one test was run from midnight until filter change at approximately 9:00 AM.

Figure 1 is an illustration of the setup of the various sampling equipment around the cattle feedyard. The only difference between the two sampling trips were the locations of the TEOM. This is indicated on the graph. The prevailing wind direction for the feedyard during both sampling trips was approximately from the southwest to the northeast. This is the reason for two sampling locations on the north side of the feedyard.

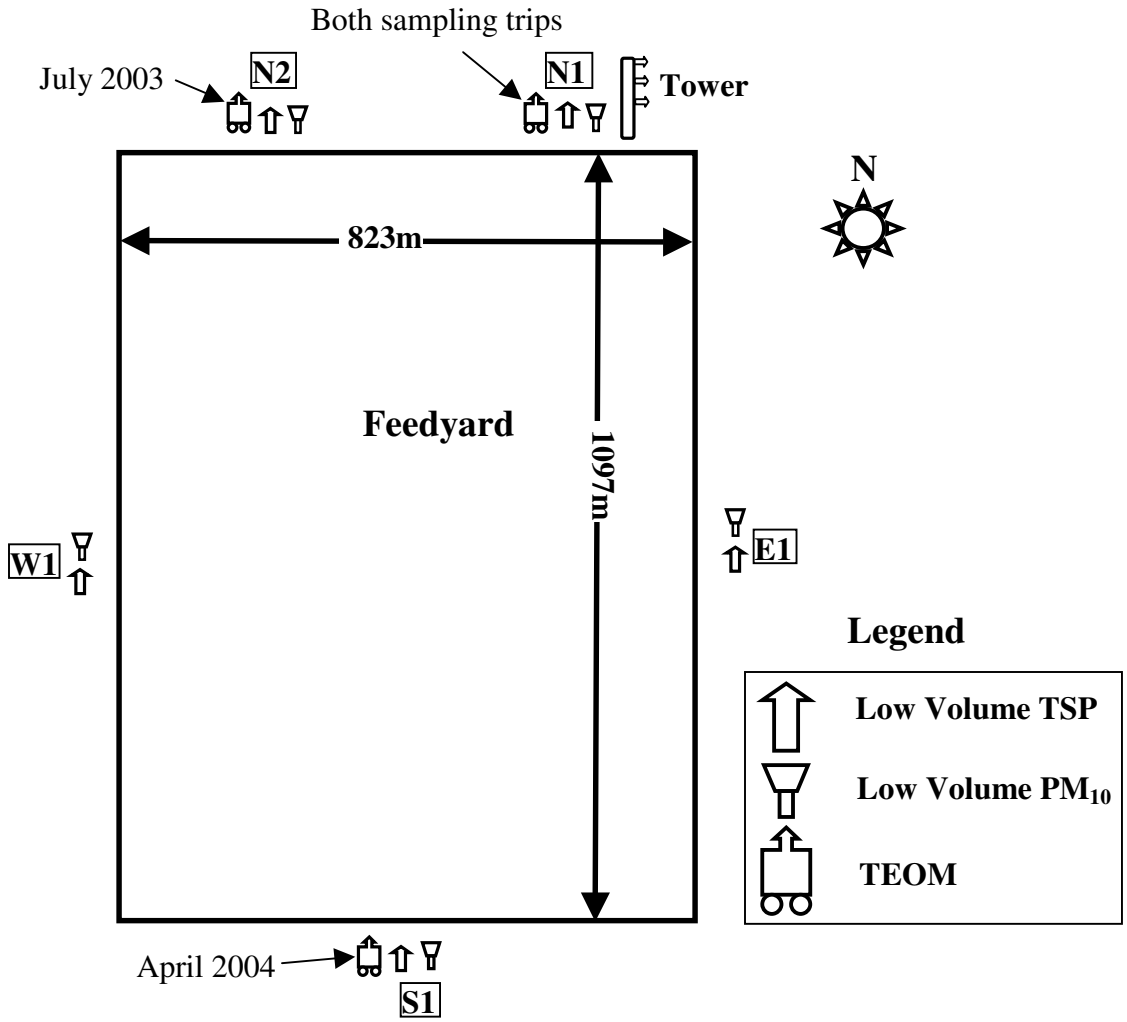

Figure 1. Schematic of the feedyard with sampler locations marked with designated symbols. The different TEOM placements for the two sampling trips are indicated by an arrow and the appropriate date.

The exposed filters were placed in sterile containers and transported back to the laboratory at Texas A&M. The particulate matter concentrations were calculated according to the procedure described by Wanjura et al. (2003). In summary, the filters were pre- and post-weighed three times using a precision analytic balance (AG245, Mettler-Toledo, Greifensee, Switzerland). The mean of each set of three weights was used as the weight of the filter. The difference in these two averages was the weight of the particulate matter captured on the filter.

By measuring the pressure drop across the orifice, flow rate through the filter can be calculated by using the orifice meter equation, shown in Equation 1.

$$Q = 3.478 * k * (D_0)^2 * \sqrt{\frac{\Delta P_a}{\rho_a}} \quad (1)$$

where Q = Volume of air, m^3/s;

k = Orifice meter constant;

D_0 = Diameter of the orifice, m;

ΔP_a = Measured pressure drop across the orifice, mm H_2O; and

ρ_a = Mean air density , kg/m^3.

The pressure drop across the orifice meter was measured using a differential pressure transducer (PX274-30DI, Omega, Stanford, CT) and a magnehelic pressure gauge (Magnehelic, Dwyer Instruments, Mich. City, IN). The pressure transducer converted pressure readings to electrical current with a range of 4-20 mA. Pressure readings were recorded by the HOBO data loggers at twelve second intervals. Another parameter needed in the orifice meter equation is the density of the air passing through the filter. This was calculated using Equation 2.

$$\rho_{ma} = \frac{P_b - P_{wv}}{0.0028 * (t_{db} + 273)} + \frac{P_{wv}}{0.0046 * (t_{db} + 273)} \quad (2)$$

where ρ_{ma} = Density of moist air, kg/m^3;

P_b = Barometric pressure, atm;

P_{wv} = Water vapor pressure, atm; and

t_{db} = Dry bulb temperature, ºC.

The orifice meter equation was also used to ensure that 1 m^3/hr was maintained during the sampling period. All orifice meters were calibrated prior to each sampling trip.

Magnehelic differential pressure gauges were used for setting the sampler to the correct pressure drop and for redundancy. Pressure readings were recorded at the beginning and end of each test period as a backup in case problems were encountered with the HOBO data recording system.

Equation 3 was used for calculating the average concentration for each test period using the appropriate inputs.

$$C = \frac{M_{PM}}{V_{air}} \tag{3}$$

where C = Mass concentration in micrograms per cubic meter;

M_{pm} = Mass of particulate matter on filter, μg; and

V_{air} = Volume of air that passed through the filter for a given test period, m^3.

The 10 m tower was located at the N1 sampling location, while the weather station was located at the predominantly upwind location at the south end of the feedyard. The tower's purpose was to determine a vertical concentration profile corresponding with a vertical wind velocity profile. It was placed at the predominant downwind edge of the feedyard for this reason.

The TEOM sampler senses the mass collected on the filter by measuring the frequency at which the tapered element oscillates. When mass accumulates on the filter during sampling, the oscillation frequency decreases. The microprocessor calculates the difference in oscillation frequency, and compares it to the normal oscillation of the

tapered element and filter cartridge at the time that the instrument was initialized. This change in oscillation is proportional to the change in mass on the tapered element.

To calculate the concentration averages, the TEOM senses concentrations every two seconds and a smoothing method is used to obtain the averaged concentrations. The smoothing method functions by averaging the frequency of the tapered element for every 10 sets of 2 second concentration measurements. An exponential smoothing routine is then applied to compute a new smoothed mass value every 2 seconds (Rupprecht and Pataschnick Co., 2002). The averaged concentration measurements are updated by these smoothed values. The TEOM samplers were not used for concentration measurement values, but as a relative measure of the daily pattern of concentration changes.

EMISSION FLUX CALCULATION

To aid in the determination of the mass flux emissions from the feedyard, the EPA-approved Gaussian-based dispersion model Industrial Source Complex Short Term Version 3 (ISCST3) was used (Trinity, 2002). ISCST3 is one of the dispersion models used by SAPRA to determine property line concentrations resulting from emission sources (CFR, 2003).

The ISCST3 interface program used for this research was Breeze©, developed by Trinity Consultants (2002). To back-calculate emission rates using ISCST3, meteorological data, gathered using the HOBO weather station (Onset Computer Corp., Bourne, MA), were used as input into the program. The protocol used for determining the emission flux for this research was described by Wanjura et al. (2004). The following list summarizes this protocol.

1. The locations and heights of the receptors (samplers) were used as input into ISCST3. The dimensions (length, width) and locations of the sources and samplers were included as input into ISCST3.
2. The duration of test periods were rounded to the nearest hour, and the meteorological data corresponding to the test periods were divided into segments equivalent to the rounded number of test hours.
3. The wind direction and speed data gathered by the HOBO weather station were vector averaged in compliance with the procedures set forth by the EPA (USEPA, 2000).
4. The segments of meteorological data that corresponded to each hour of a specific test were included as input into ISCST3.
5. An initial emission rate or flux was provided as input and the model was run to estimate concentrations that corresponded to each receptor.
6. The averages of the initial concentration values obtained in step 5 for each sampler location were compared. It was assumed that the upwind sampler was the receptor that had the lowest concentration value, and the downwind sampler was the receptor with the highest concentration value.
7. The upwind measured concentrations were subtracted from the downwind measured concentrations to obtain average net concentrations for each test.
8. The test durations for each measured concentration did not always match the rounded number of test hours as calculated in step 2. To compensate for this, it was necessary to adjust the measured concentrations using the power law with a p-value of 0.17

(Wark et al., 1998) in order to normalize them to a common time period. The power law is shown in Equation 4.

$$C_N = C_M * \left(\frac{T_M}{T_N} \right)^{0.17} \quad (4)$$

where C_N, C_M = normalized and measured concentrations, respectively, $\mu g/m^3$,

T_M, T_N = actual measurement duration and normalized duration, respectively, min.

9. The fluxes necessary to match the normalized concentrations were calculated using a direct ratio approach. This ratio approach is derived from the Gaussian equation (Cooper and Alley, 2002), which is shown in Equation 5.

$$C = \frac{Q}{\pi \times u \times \sigma_y \times \sigma_z} \times \exp\left(-\frac{1}{2} \frac{y^2}{\sigma_y^{\,2}} \right) \times \exp\left(-\frac{H^2}{2 \times \sigma_z^{\,2}} \right) \quad (5)$$

where C = concentration predicted at a certain distance downwind of a source, $\mu g/m^3$;

Q = emission rate of the source, $\mu g/m^2$-s;

u = wind velocity, m/s;

σ_y, σ_z = horizontal and vertical dispersion parameter, respectively, meters;

y = receptor distance from downwind centerline, meters; and

H = emission source height, meters.

The concentrations resulting from the initial flux are compared to measured concentrations, so that the emission rate necessary to produce the measured concentration can be calculated. The Gaussian equation (Equation 5) can be simplified for this calculation, because the only variables changing are the emission rates, Q, and the

concentrations, C. The resulting equation used to calculate the emission rates required to produce the measured concentrations is Equation 6.

$$\frac{Q_1}{Q_N} = \frac{C_1}{C_N} \tag{6}$$

where Q_1, Q_N = fluxes to match initial and normalized concentrations, g/m^2-s; and

C_1, C_N = initial and normalized concentrations, $\mu g/m^3$.

To calculate the average daily flux, the fluxes for each test period were categorized into one of three categories: night, day, and 'peak'. To calculate the average flux for each category, all of the fluxes that occurred during each category were time-averaged. Time averaging was accomplished by taking the flux for each test in a category, multiplying it by its duration, summing all such calculations for a category together, and then dividing this total sum by the total number of hours for the category.

EVENING DUST PEAK ANALYSIS

ISCST3 was utilized to determine the effect of the meteorological conditions on the measured concentrations downwind. Table 1 lists the meteorological conditions that ISCST3 required to calculate mass concentrations. The meteorological data were collected every two minutes at the feedyard using the HOBO weather station (H21, Onset Computer Corp., Bourne, MA). The wind speed and direction were vector-averaged into one-hour averages according to the guidelines set forth by the EPA (USEPA, 2000). The rest of the meteorological conditions except mixing height were averaged into one-hour averages. All of the one hour averages were provided as input into ISCST3.

The mixing height was the only meteorological condition in Table 1 that was not measured at the feedyard. Mixing height is defined by Holzworth (1972) as *the height*

above the surface through which vigorous mixing occurs. Mixing height can potentially increase concentration by effectively reducing the volume of air into which the PM emissions disperse. For the mixing height in this study, only the rural mixing height was used. The rural and urban label refers to the surface roughness, i.e. an urban area having more surface roughness due to the presence of buildings.

Table 1. Listing of the meteorological conditions used by ISCST3 to calculate mass concentrations.

Wind speed
Wind direction
Ambient Temperature
Stability Class
Mixing Height – rural and urban

A comparison of concentrations was performed using measured meteorological data from the July 2003 and April 2004 trips. The meteorological conditions associated with the tests during which the evening dust peaks occurred were provided as input into ISCST3, along with the 24 h average flux excluding peaks for both tests. The mixing height was placed at 1000 m used by ISCST3 so the effect of changes in wind speed and stability class on concentrations can be observed and recorded while not being affected by mixing height. This procedure was performed for each of the evening dust peaks, and the concentrations that ISCST3 predicted for each of the evening dust peaks were recorded and compared to the concentrations actually measured during the evening dust peaks. The percent difference between the predicted concentrations and measured concentrations was calculated and recorded. This calculation was performed to quantify

the effect of changes in wind speed and stability classes on the concentration measurements downwind.

ISCST3 was used to predict the effect that the mixing height may produce upon concentrations downwind. An arbitrary emission rate was used, and every meteorological condition remained constant except for the mixing height. The mixing height started at 80 m and decreased by increments of 5 m until the height of 5 m was reached. The concentrations that were the result of each change in mixing height were observed and recorded. This procedure was repeated for stability classes of A, C, D, and F with an average wind speed according to Cooper and Alley (2002) for each stability class was used as input into ISCST3. This was to determine the effect the mixing height had combined with various stability classes on concentrations predicted downwind. Also, the average stability class and wind speed measured by the meteorological station during both sampling trips was combined with changes in mixing height to determine the how much of the concentration increase in the evening could be attributed to the mixing height.

ROAD AND FEEDLOT CONTRIBUTION ANALYSIS

During the April 2004 feedlot sampling trip, a unique event allowed new information about the origin of fugitive PM emissions from a cattle feedyard to be collected. Rain events up to two days prior to the beginning of the sampling trip saturated the surface of the feedlot. Work by Parnell et al. (2003) indicates that PM emissions from a feedlot are reduced to almost zero for several days after a significant rain event. After two days, the sources of fugitive PM emissions begin to emit, but at

very reduced levels from normal. Although the feedlot pen surface moisture conditions were not measured during the April 2004 sampling trip, the emissions from the pen surfaces were observed to be drastically reduced compared to previous sampling trips. The road emissions were observed to increase more rapidly than the pen surface. Wanjura et al. (2004) concluded that the majority of the concentrations measured at the feedyard during the April 2004 sampling trip were due to road emissions. Different surface characteristics of the pen surface versus the unpaved roads are likely to account for the difference in decreased emission rates due to the rain events.

To determine the contributions that road and pen surface emissions have on downwind concentrations, it was necessary to separate the feedyard from the roads. The procedure used in this study utilized ISCST3 to model the feedyard and road emissions separately. Figure 2 was the setup used in ISCST3 to calculate the comparison between the feedyard and the roads.

The roads passed completely around and through the feedyard. It was assumed that the average width of the vehicles passing along the roads was three meters, because the vehicles traversing the feedyard were most likely to be pickup trucks, 20-ton feed trucks, or eighteen-wheelers (semis) loading or unloading at the feedmill at the north end of the feedyard. The roads were modeled as line sources. The cattle pens were modeled as area sources, but separated so that the roads could pass between the pens. Figure 2 depicts the setup used in ISCST3 to determine the contribution difference between the roads and pen surfaces.

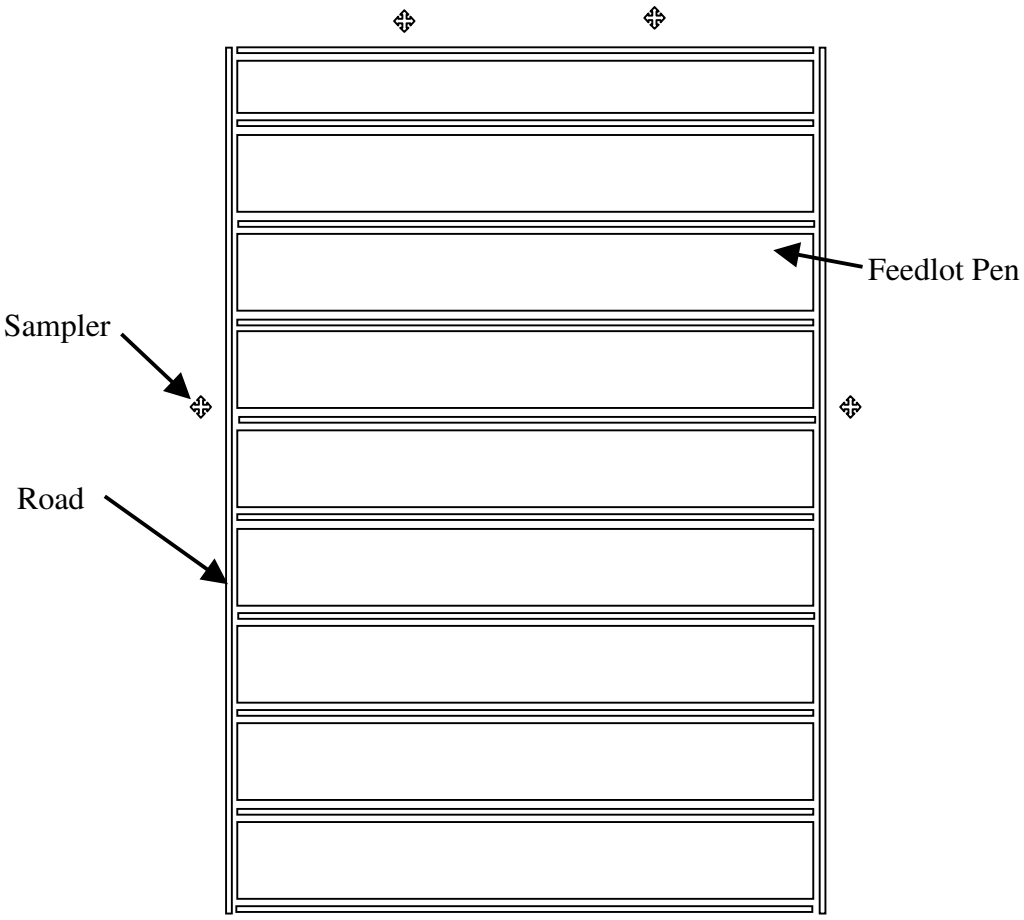

Figure 2. Illustration of the ISCST3 layout of the feedyard with the various sources indicated. The narrow, long sources are the roads, whereas the larger, rectangular shapes are the feedlot pens. The crosses on the illustration represent the sampler locations around the feedyard. The feedyard is approximately 1134 by 835 meters, with the roads 10 meters wide. All of the pens except the top one are 122 by 835 meters, with the top being 61 by 835 meters.

The emission factor used for comparison to the unpaved road emission factor developed by Wanjura et al. (2004) was that prepared by the USEPA in its AP-42 emission factor document. The unpaved road emission factor was divided into two different categories: industrial and public. The industrial emission factor is described as those roads predominantly used by heavy duty vehicles, while the public emission factor is associated with roads dealing with light duty traffic. Because the majority of the traffic on the feedyard was heavy equipment, semis, and feed trucks, the industrial emission

factor was considered to be the more appropriate of the two. The industrial emission factor was calculated using Equation 7, which is the emission factor equation from the EPA's AP-42 document.

$$EF = k(s/12)^a (W/3)^b \quad (7)$$

where EF = size specific emission factor, lbs/vehicle-mi traveled,

s = surface material silt content, percentage;

W = mean vehicle weight, tons; and

k, a, and b are empirical constants, determined by the emission factor's particulate matter size. Values for the PM_{10} emission factor are k = 1.5, a = 0.9, and b= 0.45.

The emission factor was converted to a form that ISCST3 could use. The line source used by ISCST3 requires that the emission rate be in grams per square meter per second (g/m^2-s). This is confusing, as line source algorithms usually require emission rates in mass per length per time. The conversion to the ISCST3 required emission rate is accomplished using Equations 8 and 9.

$$Area\ Flux = \frac{EF \times VMT_{total} \times 454}{L \times W \times t_{truck}} \quad (8)$$

where Area Flux = amount of PM_{10} the truck produces per unit area, g/m^2-s;

EF = AP-42 emission factor for unpaved roads, lbs/VMT;

VMT_{total} = total vehicle miles traveled, miles;

L = length of road that the trucks travel, m;

W = width of the roads, m;

t_{truck} = time necessary for a vehicle to travel the distance, seconds; and

454 is the factor to convert pounds to grams.

To calculate t_{truck}, Equation 9 was used.

$$t_{truck} = \frac{VMT_{total}}{S} \times 3600 \quad (9)$$

where t_{truck} = time it takes for a truck to travel its path, seconds;

S = speed of the truck, mph;

3600 = factor to convert hours to seconds; and

VMT_{total} = vehicle miles traveled by a truck.

Because the line sources for each alley and perimeter road were individual, it was possible to discriminate between the different roads and the amount of traffic that passes over each one. For simplification of applying the AP-42 emission factor, several assumptions were made:

- Only feed trucks were used in this experiment.
- The width of the line source emissions was assumed to be the same as the width of the roads, which was ten meters. Even though the width of the vehicle traffic was assumed to be 3 m, the passage of a vehicle introduces interaction of air with the road surface.
- The average truck speed was 8 kmph, which is representative of the average speed of the feed trucks.
- Vehicle weight was assumed to be 18.1 metric tons, representing the weight of the feed trucks and eighteen wheelers traveling the roads.

The measurement of the silt content was done by taking a sample of the road surface material, and passing it through a set of sieves to measure the silt content. Silt content is defined by the AP-42 as *particles smaller than 75 micrometers in diameter* (USEPA, 2003). The fraction is calculated by "measuring the proportion of loose dry

surface dust that passes a 200 mesh screen, using the ASTM-C-136 method" (USEPA, 2003). Table 2 is percentages derived from samples taken at various points on the roads of the feedyard.

Table 2. Listing of the silt content percentages derived from samples gathered at locations around the feedyard. The silt content percentage is coupled with the location of its sampling site.

Location	Silt Content, %
North	4.92
East	2.62
West	3.01
South	11.13

In order to determine how different silt contents affected the calculation of the unpaved road emissions fluxes, three silt contents of 5, 10, and 15% were chosen as a range representative of the silt content of the unpaved roads on the feedyard. These silt contents were used as input into the AP-42 method (Equation 6) to determine three emission factors. These emission factors were converted to emission fluxes using Equation 7.

To determine the distance used for VMT_{total}, the number of feed alleys on the feedyard was multiplied by the length of the feed alleys to calculate the distance traveled in the feed alleys. It was necessary to add the distance necessary for the trucks to reach the feed alleys to obtain a total distance. To calculate the distance traveled on the two access roads a total of ten trips were multiplied by half the length of one of the access roads to obtain an average of the distance traveled on one of the access roads. This value

was doubled to obtain the distance traveled on the access roads and added to the distance traveled in the feed alleys to obtain the total miles traveled by the feed truck. This value was used in Equations 7 and 8.

The emission fluxes calculated from the AP-42 method were combined with a constant emission flux of 6.8 kg/1000hd-day for the pen surface (Parnell et al., 1999). This set of emission rates was combined with a meteorological data set that was designed to provide a range of stability classes and wind speeds. This meteorological data set is shown in Table 3. The purpose for this analysis was to demonstrate the effect of different silt contents, stability classes, and wind speeds on concentrations predicted downwind using ISCST3.

Table 3. Set of meteorological data representing the range of stability classes and related wind speeds used for modeling. Each of the three unpaved road emission fluxes were combined with the pen surface emission flux and each stability class and wind speed represented in the table to calculate concentrations downwind. The wind direction was from the south.

Wind Speed (m/s)	Day Stability Class	Night Stability Class
1.5	A	F
2.5	B	E
4	B	E
5.5	C	D
6	C	D

Another analysis was used to determine the road emissions necessary to produce concentrations measured at the feedyard. The emission rate associated with cattle activity (pens where cattle were confined) was set at a constant 6.8 kg/1000 hd-day. Four sets of measured meteorological data, two from each sampling trip, were used to approximate the required road emission rates based on the average measured concentration from each of the 4 tests. The meteorological data sets were chosen from daytime test periods that occurred during the morning (0600 – 1200). The reason for this choice was to omit drastic changes in meteorological conditions e.g. those that occur during the evening dust peak. Night tests were not selected because unpaved road traffic at night was limited and would not provide representative results for the road emissions.

The Figure 2 setup was utilized in this procedure as well. An initial flux was used as input for the road emission rate and the resulting predicted concentrations were recorded. The road emission flux necessary to produce the measured flux was calculated using a ratio method similar to the one described by Equation 6. It was necessary to include the area of the feedyard and roads, however. Equation 10 was the derivation of the ratio used to calculate the required road emission flux to match the measured concentrations.

$$Q_{r,req} = \frac{(C_m - C_p) \times Q_f \times A_f + C_m \times Q_{r,arb} \times A_r}{A_r \times C_p} \qquad (10)$$

where $Q_{r,\,req}$ = Emission flux for the roads required to produce the measured concentrations, g/m^2-s;

C_m = Average concentration measured during the test period, µg/m^3;

C_p = Average concentration predicted for the test period using measured meteorological data and $Q_{r,\,arb}$, µg/m^3;

Q_f = Emission flux for the feedlot surface, g/m^2-s;

A_f = Area of the feedlot, m^2;

$Q_{r, arb}$ = arbitrary flux input into ISCST3, g/m^2-s; and

A_r = Area of the roads, m^2.

SCIENCE BASIS FOR ISCST3 AREA SOURCE

According to the manual for ISCST3 (Trinity, 2000), the calculation of concentrations downwind of an area source is estimated using a line source algorithm. The specific mechanics of producing the concentrations using the line source algorithm are unclear. However, it (the manual) does explain that the area source is divided into lines, and that the contribution to the concentration prediction downwind is calculated for each line. All line contributions are summed to produce the total concentration.
An attempt to model an area source based on the Infinite Line Source Algorithm (ILSA) was performed and recorded by Hamm et al. (2005). This procedure employed the ILSA by splitting the area source into equal widths and using the resulting "lines" dimensions as inputs.

Based on this procedure, the modeling of a feedyard including unpaved roads was done. For comparison, the feedyard schematic (Figure 2) was used as input into ISCST3 using specified emission rates for the unpaved roads and pen surfaces. The emission rate used for the feedyard was 6.8 kg/1000 hd-day, developed by Parnell et al. (1999). This was converted to an emission flux using a cattle spacing of 13.9 m^2/hd (Wanjura et al., 2004). The road emission rate used was the same emission rate calculated using 5% silt content.

The ILSA required that the emission rate be in terms of mass per length per time rather than mass per area per time. The feedyard pens shown in Figure 2 were divided into 10 m deep 'lines' to match the depth of the roads. Depth refers to the dimension of the line perpendicular to the receptor. The area emission flux was then multiplied by the area of the line, and then divided by the length. The resulting emission rate was used in the ILSA as Q_L, shown in Equation 11.

$$C = \frac{2Q_L 10^6}{\sqrt{2\pi}(\sigma_z u)} e^{\left(-\frac{1}{2}\left(\frac{H}{\sigma_z}\right)^2\right)} \quad (11)$$

where C = concentration at some distance downwind, $\mu g/m^3$;

Q_L = line emission rate, g/m;

σ_z = vertical dispersion parameter, meters;

u = wind speed, meters per second; and

H = effective emission height, meters.

The σ_z component was calculated for the above equation by using Equation 12.

$$\sigma_z = aX^b \quad (12)$$

where X = downwind distance to the sampler, kilometers; and

a and b are constants that are dependent upon stability class (Turner, 1994).

Typical values for stability class "D" are a = 34.5 and b = 0.870

To compare ISCST3 and the ILSA, a simple set of meteorological conditions was used:

- Wind direction was always from the south;
- The receptor was in the center of the north side of the feedyard, located 10 m downwind;

- Stability class D with an average wind speed of 5 m/s.

The results of ISCST3 and ILSA were compared to note any similarities between the two models.

RESULTS

CONCENTRATION MEASUREMENTS

TSP and PM_{10} concentration measurements upwind and downwind from fugitive sources of PM at an operating feedyard were essential to achieve the objectives of this research. PM concentration measurements during the July 2003 trip provided data used to quantify PM emissions of feedyards experiencing unusually hot and dry conditions. When the sampling took place, a rain event had not occurred in several weeks so the emissions from the feedyard were abnormally high. PM concentration measurements during the April 2004 trip provided data used to quantify PM emissions from feedyards immediately following significant rainfall events. The April 2004 sampling provided data that allowed for quantification of PM emissions associated with vehicle traffic (road emissions) in contrast to cattle activity (pen surface emissions). Step function increases and decreases in PM concentrations at sun down referred to as "evening dust peaks" were observed for both July 2003 and April 2004 sampling trips. The concentration data for the two significantly different feedyard conditions provided the basis for an engineering analysis of the evening dust peak phenomenon. It has been hypothesized by some (Mitloehner, 1999) that evening dust peaks were solely attributed to increased cattle activity with the quick and significant drop in temperature at sun down.

The July 2003 trip occurred during a hot and dry period. Temperatures ranged from 38°C in the daytime to 21°C at night. With very little moisture content in the feedlot pen surface, the emissions from the feedlot were noticeably high. During this trip, the large magnitude of the change in concentrations during the evening dust peak became apparent. The net concentrations calculated from this trip ranged from 113 to

6000 μg/m^3. The actual timing of the change in concentrations followed a similar pattern noticed by researchers in the past (Parnell et al., 1993; Auvermann, 2001). The concentrations peaked in the evening, approximately the time the temperature and solar radiation decreased. The lowest concentrations were found early in the morning, prior to sunrise.

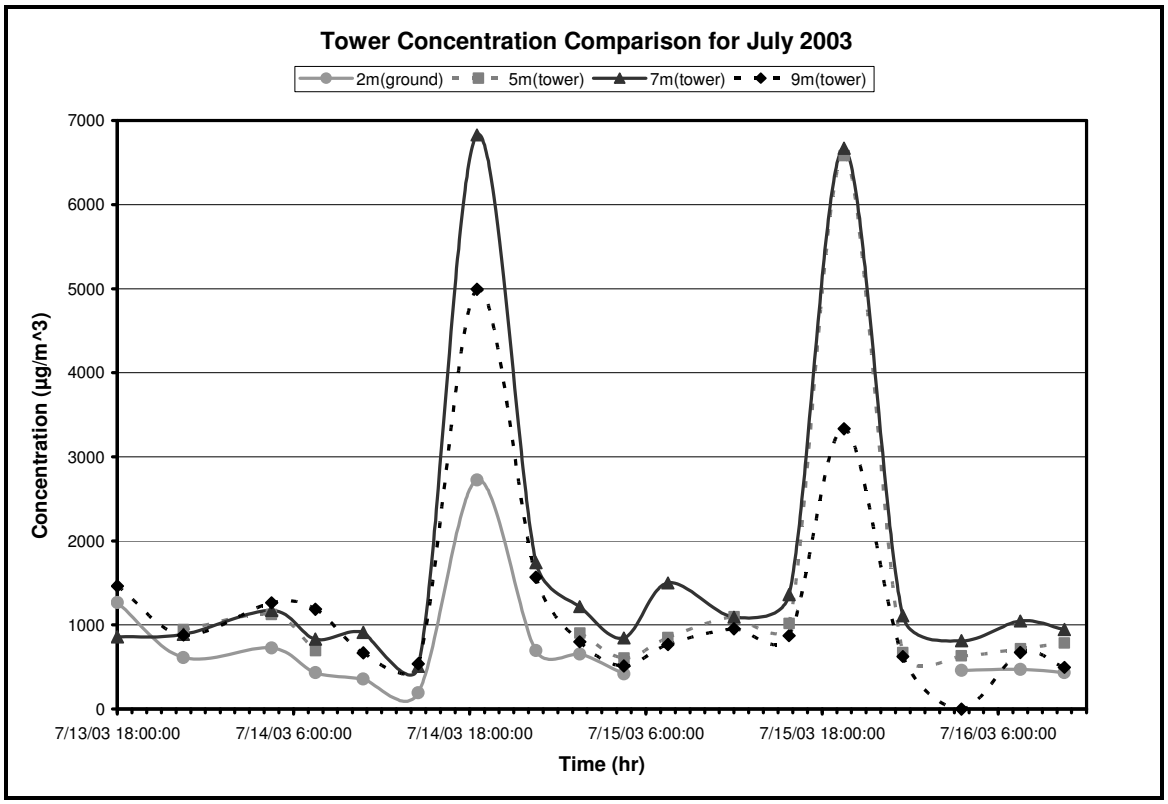

Figure 3. July 2003 average TSP concentration measurements from the 10 m tower designated by a data point for each test period. The points are located at the time of the start of each test. Missing values for the 2m and 5m samplers were the result of equipment failures.

The daily concentration fluctuation is shown in Figure 3. The TSP concentration measurements shown in Figure 3 were taken from the tower located at N1. The 2 m

sampler measurements were taken from the ground-level sampler. The 5 and 7 meter concentration measurements in Figure 3 were noticeably higher than the 2 and 9 meter measurements during the two evening dust peaks. This suggests that the maximum concentration for the July 2003 sampling trip would be measured between 5 and 7 meters.

Table 4 lists the emission fluxes calculated from the July 2003 sampling trip. For the July 2003 sampling trip, sampling test periods that occurred between 2300 and 0730 were considered to be night tests. Day tests were considered to occur between 0730 and 1900, and the evening peak tests were those that occurred between 1900 and 2300. The concentrations for each of these tests were back-calculated into emission fluxes using the procedure described in the Methods section. The fluxes corresponding to day, night, or evening dust peak were averaged to obtain an average TSP emission flux for each of these three time periods. The resulting day, night, and evening peak fluxes were weighted and averaged to obtain a 24-h average flux including peaks. This average 24-h emission flux was based on the hypothesis that cattle activity is the sole source of the PM concentration changes during the evening dust peaks. To obtain an average 24-h emission flux excluding evening dust peaks, just the day and night fluxes were weighted and averaged. This 24-h emission flux was based on the hypothesis that the concentration increases in the evenings were due solely to meteorological conditions. This would mean that the emission flux during the evening dust peak remained constant and did not increase from the average 24-h emission flux excluding peaks.

Table 4. TSP emission fluxes calculated using ISCST3 for the July 2003 feedyard sampling trip. The fluxes are separated into day, night, and peak fluxes. The 24 hour average with and without peaks are to show the effect of the evening dust peak on the flux calculation.

Flux type	Average TSP Flux ($\mu g/m^2$-s)
Day	79.4
Night	35.2
Peak	192
24-h average with peaks	99.1
24-h average without peaks	60.6

The TEOM hourly concentrations (Figure 4) provided a more detailed pattern of PM concentrations than did the gravimetric sampler data. The TEOM concentration measurements were not used in the calculation of the average 24-hr emission fluxes. Instead, they were used to provide a relative measure of the daily concentration patterns. TEOM concentration versus time data provided the ability to more accurately observe the specific times associated with start and ending of evening dust peaks, due to a higher time resolution.

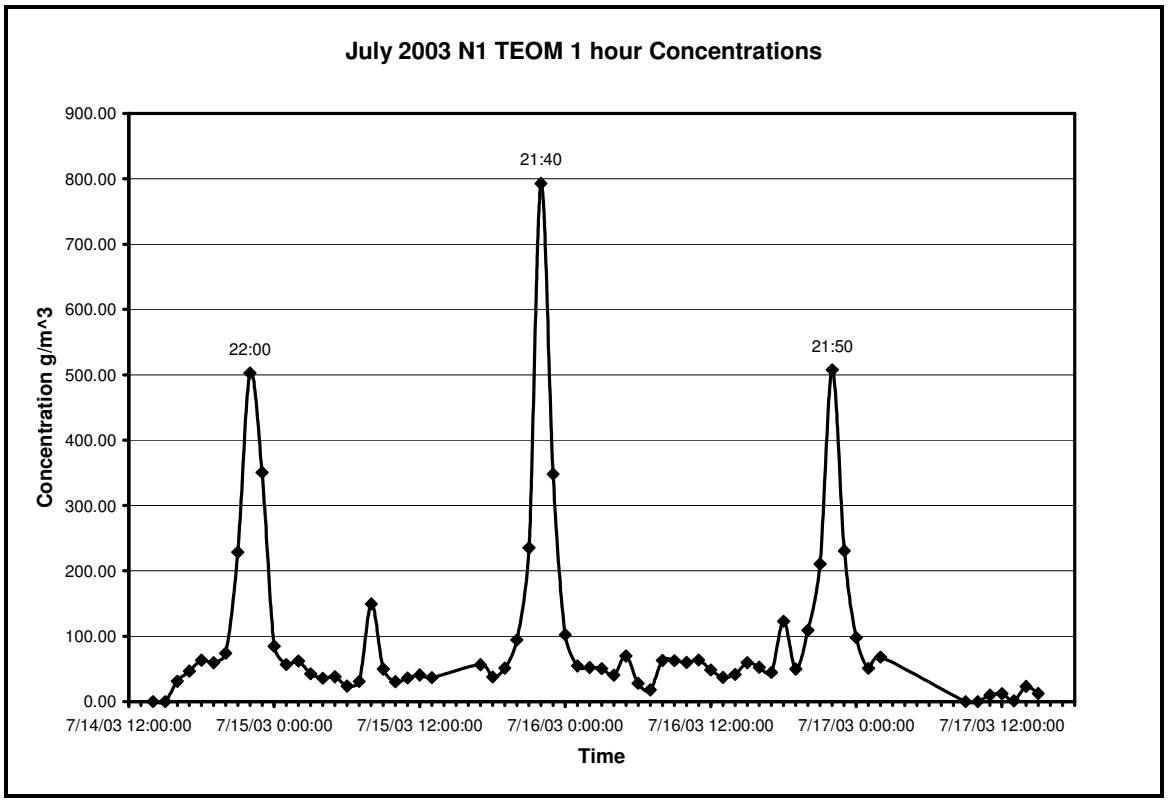

Figure 4. Hourly concentrations measured by the TEOM located at the North 1 location during the July 2003 sampling trip. The times indicated above the spikes are the peak times according to the TEOM 10 minute concentration data.

The TSP concentrations from the April 2004 sampling trip measured by the tower followed a daily pattern similar to those from the July 2003 trip. Figure 5 illustrates this pattern over the series of tests. There are four evening dust peak events depicted on the graph. The feedlot had experienced a rain event the week prior to the sampling trip. Much of the pen surfaces remained wet. In contrast, the unpaved road surfaces held little moisture and dried quickly when exposed to rainfall. It must be noted that the evening dust peaks occurred, on this sampling trip in spite of the fact that the moisture contents of the cattle pen surfaces were high and the PM emission rates from these surfaces were

low. This observation suggests that the evening dust peaks are not due solely to increased cattle activity. The cattle activity may be increased in the evening, but the increases in concentration are due, at least in part, to another factor, most likely meteorological conditions.

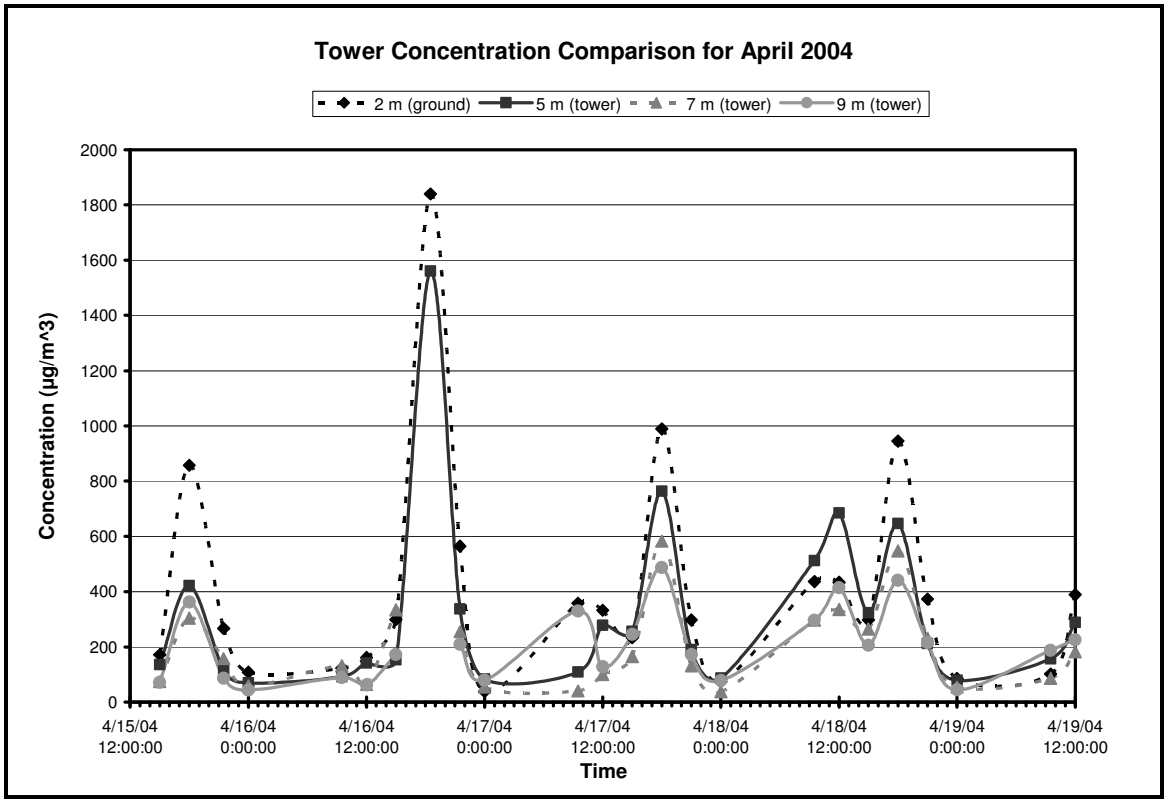

Figure 5. April 2004 hourly TSP concentration measurements for each test period from the 10 meter tower set up at the North 1 location. The test periods are matched approximately with the time that each specific test period started. Missing data points are the result of equipment failures.

As with the July sampling trip, the TEOM concentration versus time data provided more precise determinations of when evening dust peaks started and stopped. Figure 6 shows the hourly concentrations recorded with the TEOM sampler during the April 2004 trip. Data from the TEOM samplers indicated that the evening dust peaks occurred within approximately 10 minutes of 21:00 each day. The occurrences of the evening dust peaks during the April 2004 sampling trip are important because the feedlot pen surface emissions should have been very low due to surface moisture conditions. Wanjura et al. (2004) concluded that the primary source of PM emissions during the April 2004 sampling trip were from the roads. Evening dust peaks depicted in the April 2004 TEOM data (Figure 6) occur at the same time relative to sunset as the July 2003 TEOM data (Figure 4).

The occurrence of the evening dust peak in July 2003 suggests that cattle activity could be responsible for the increase in concentrations due to the evening dust peak. The rain event in April 2004, however, decreased the pen surface emissions therefore reducing the effect of cattle activity on concentrations. There were similar evening dust peak concentration increases in the April 2004 sampling trip as in the July 2003 sampling trip. In order for cattle activity to be the sole source of evening dust peaks, the PM emissions must originate from the pen surface where the cattle are located. Without the PM from the pen surface, it is unlikely that an evening dust peak would occur, based on the hypothesis that cattle activity are the sole source of the evening dust peak. The only other source of fugitive PM emissions on a feedyard are the unpaved roads, but road traffic was negligible at the times corresponding to the evening dust peaks for the April

2004 trip. Therefore, it is unlikely that cattle activity is the sole source of the evening dust peak.

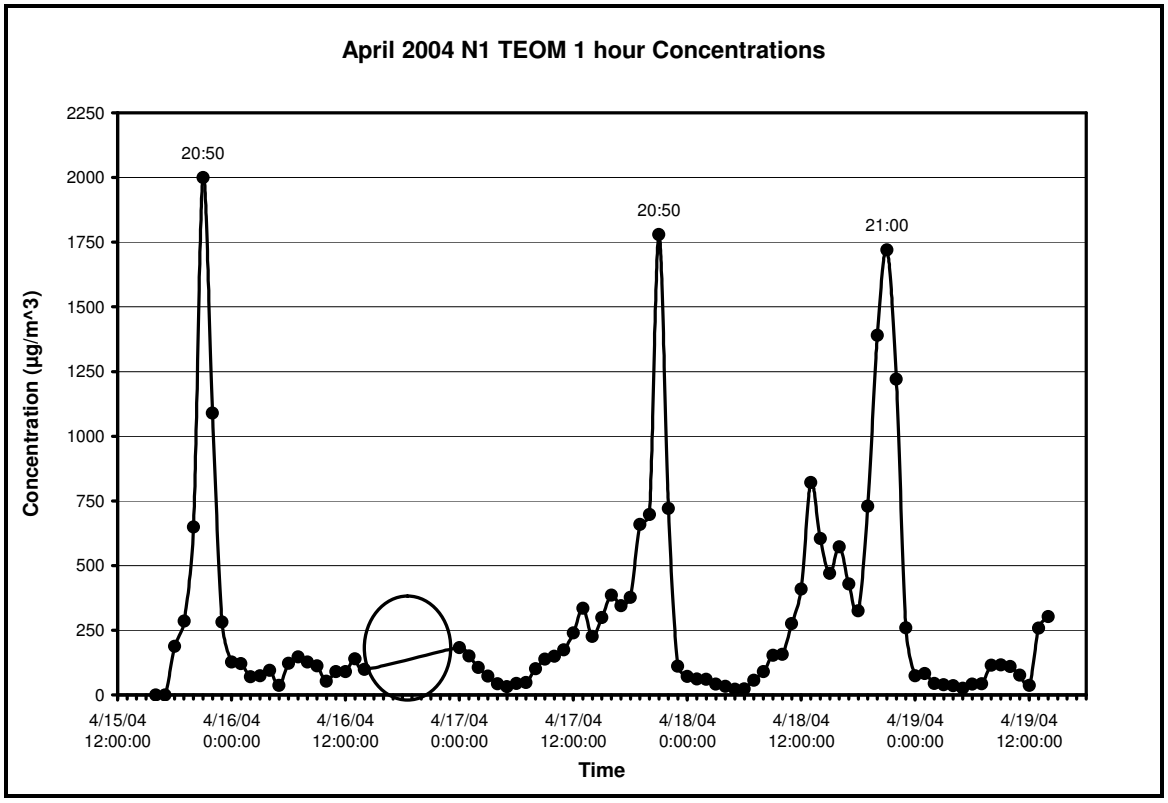

Figure 6. Hourly concentrations measured by the TEOM located at the North 1 location during the April 2004 sampling trip. The time of the peak occurrence is shown above each peak. The second peak, indicated by the circle, is not on the graph due to equipment problems.

For the April 2004 sampling trip, the evening peak period occurred from 1800 to 2100. The night period was the sampling tests that transpired from the end of the evening dust peak until nine in the morning. The day period occurred from 0900 until 1800. The calculation of the 24-h average daily fluxes including and excluding evening dust peaks was performed in the same manner as the July 2003 calculations.

Table 5 displays the various emission fluxes calculated from the TSP concentrations measured during the April 2004 sampling trip. The nighttime emission flux is lower than the July 2003 trip due to limited emissions from the feedyard (Wanjura et al., 2004). The difference in the 24 hour average fluxes including and excluding the evening dust peaks is not as pronounced as the July 2003 trip. This smaller difference may be due to overall reduced emissions.

Table 5. TSP emission fluxes calculated using ISCST3 for the April 2004 feedyard sampling trip. The fluxes are separated into day, night, and peak fluxes.

Flux type	Average TSP Flux ($\mu g/m^2$-s)
Day	106
Night	15
Peak	131
24 hr average with peaks	64
24 hr average without peaks	54

EVENING DUST PEAK ANALYSIS

The evening dust peak is a repeating event that occurs approximately the same time each evening. By taking the peak times recorded by the TEOM (these data are in ten-minute intervals) it is possible to compare to the time of sunset and related factors. Table 6 was created using data gathered by the United States Naval Observatory.

Table 6. Evening dust peak times as determined by the TEOM compared to sunset time, End of Civil Twilight, and the date upon which the peak occurred.

Date	Sunset	End of Civil Twilight	TEOM 10-min peak	Solar Radiation end time
July 14, 2003	21:01	21:30	21:30	21:06
July 15, 2003	21:00	21:29	21:20	21:00
July 16, 2003	21:00	21:29	21:40	21:04
April 15, 2004	20:19	20:45	20:50	20:21
April 16, 2004	No Data			
April 17, 2004	20:21	20:47	20:50	20:21
April 18, 2004	20:22	20:48	21:00	20:16

For these two sampling trips, the TEOM concentration peak times always occur within twenty minutes of what is called the End of Civil Twilight (ECT). Civil Twilight is a term defined by the United States Naval Observatory to "begin in the morning, and to end in the evening when the center of the Sun is geometrically 6 degrees below the horizon." (USNO, 2005) Although the ECT is not responsible for the dust peak, it can be used as a possible prediction time for when the evening dust peak will occur.

Other events that occur within the dust peak are a measured drop-off in the wind speed in the hours leading up to sunset, as well as slight changes in wind direction. Both of these events culminate at approximately the same time as that of the evening dust peak. Figures 7 and 8 illustrate the measured wind speeds as a function of time measured by the HOBO weather station. These data illustrate the occurrences of low wind speeds at times corresponding to occurrences of evening dust peaks. Only one exception occurs in Figure 8 on 4/17/2004. The reason that an evening dust peak occurs without a decrease in wind speed is unknown.

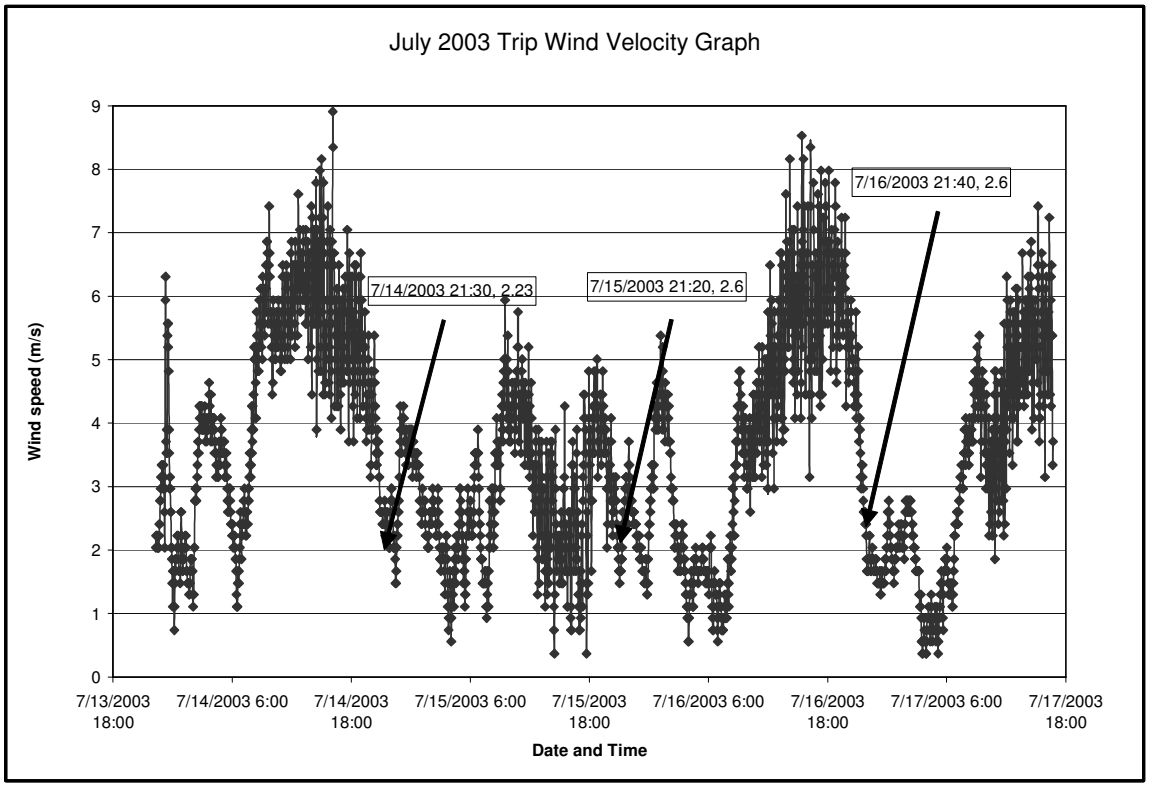

Figure 7. Wind velocity data recorded by the meteorological station upwind of the feedyard for the July 2003 trip. Noted on the graph are the evening dust peak times as well as the corresponding wind speeds.

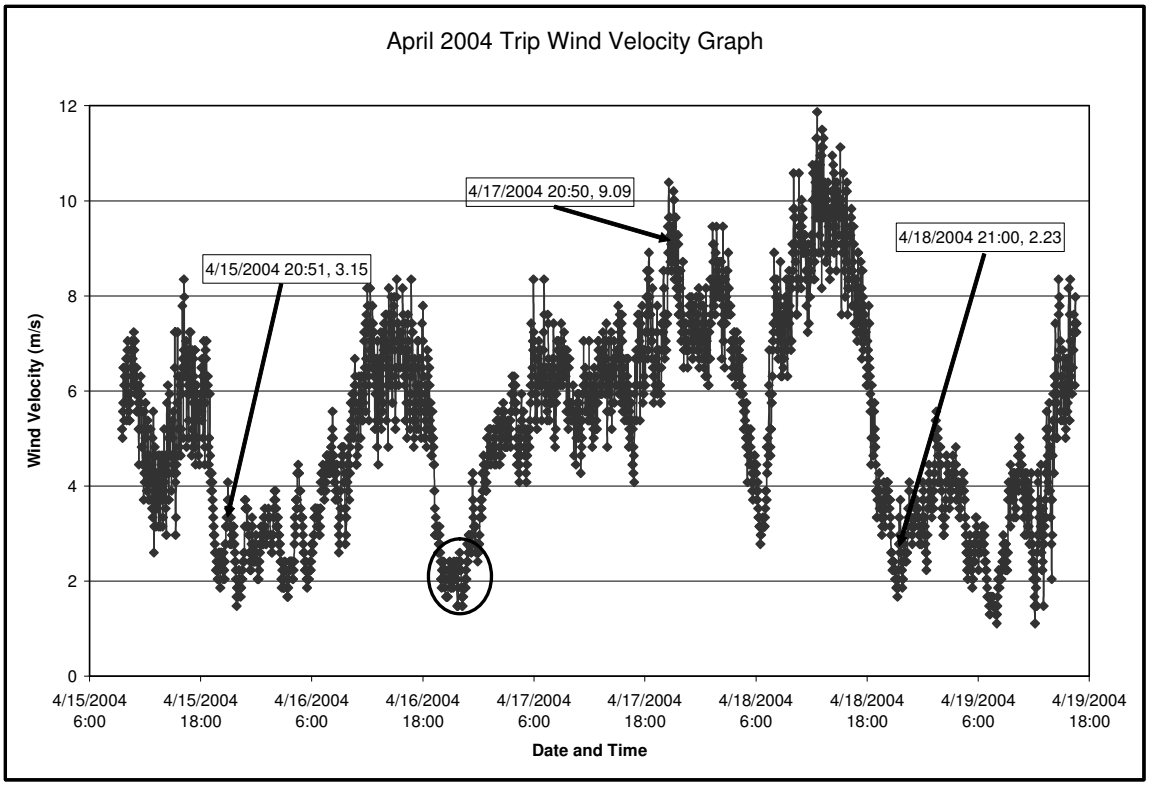

Figure 8. Wind velocity data recorded by the meteorological station upwind of the feedyard for the April 2004 trip. The circled area indicates the approximate time of the second evening dust peak.

The results for determining the possible contribution to the increased concentrations downwind as a result of changes in stability class and wind speed are displayed in Table 7. The emission flux of 60 μg/m^2-s was used, because it was approximately equal to the 24-h average flux excluding peaks that was calculated for both trips. The purpose of this analysis was to determine if changes in wind velocity and stability class measured for the evening dust peaks were responsible for the increase in concentrations. The percentages describe what portion of the measured concentrations for the North 1 ground location can be attributed to changes in wind speed and stability class measured for the peak test periods. The percentages in Table 7 suggest that it is

likely that an average of approximately 40% of the increases in concentration during the evening dust peak can be attributed to changes in wind velocity and stability class.

Table 7. Results depicting what percentage of the measured TSP concentration for the North 1 low-volume TSP location can be attributed to changes in wind velocity and stability class measured at the feedyard. The concentrations shown in the table are short term (2 to 4 hour) averages.

	Predicted Concentrations	Measured Concentrations	Percentage
July 2003			
Peak 1	1153	2366	49
Peak 2	1220	5257	23
Average			36
April 2004			
Peak 1	279	828	34
Peak 2	546	1715	32
Peak 3	460	912	50
Peak 4	467	897	52
Average			42

It was possible to take meteorological data gathered at the site and input it into ISCST3. By placing the data occurring during the evening dust peak, it was possible to recreate what happened to the concentrations due to wind velocity changes. Table 8 matches wind speed and the corresponding concentration predicted by ISCST3. The concentrations change as the wind speed and stability class change, even though the emission rates from the roads and feedyard are assumed to be constant.

Table 8. Concentrations calculated using ISCST3 and changes in wind speed and stability class recorded at the feedyard. The meteorological data used was Test 17 of the July 2003 sampling trip.

Hour	Wind Velocity (m/s)	North 1 concentrations ($\mu g/m^3$)	North 2 concentrations ($\mu g/m^3$)	West concentrations ($\mu g/m^3$)
1	5.71	390	460	363
2	4.22	565	610	476
3	2.05	1200	1250	957
4	1.58	1540	1625	1260

Table 8 illustrates each concentration's dependency upon the wind velocity. In general, the lower the wind speed, the higher the concentration.

Another possible cause for the concentration increase is that the mixing height decreases as the temperature and wind decrease during the evening. The dispersion scenario that closely matches the observed conditions is called "fanning" (Trinity 2000, Wark et al. 1998). It is a scenario that occurs when the horizontal dispersion is normal or approximately normal, but the vertical dispersion is limited or decreased. This results in the concentrations being considerably increased while the flux remains constant. This condition is illustrated in Figure 9.

The dust plume is limited vertically, shown by the observed lack of particulate matter above a certain height. The layer height in Figure 9 is indicated by the dotted line. Although the height of this layer is unknown, it appears to be between 10 to 20 m. This observation would suggest that it is likely that mixing height may also be one of the critical meteorological conditions involved with the concentration increase in the evening.

Figure 9. Photograph taken of a feedyard which depicts the layers of particulate matter that occurs in the evening period. The line differentiates the layer of high particulate matter concentrations from a layer of relatively clear air. Photo courtesy of Dr. Brent Auvermann.

Figure 10 demonstrates the relationship between concentrations and changes in mixing height when all other meteorological conditions and the emission rate remain constant. Each line in Figure 10 represents a different stability class, denoted in the legend by the prefix SC. The various stability classes react to changes in mixing height differently. Stability class "F" does not react at all, suggesting that the most stable stability class deals with the mixing height differently than the other stability classes. Stability class "A" changes the most with changes in mixing height, as does "C" and "D", but with a reduced magnitude compared to A.

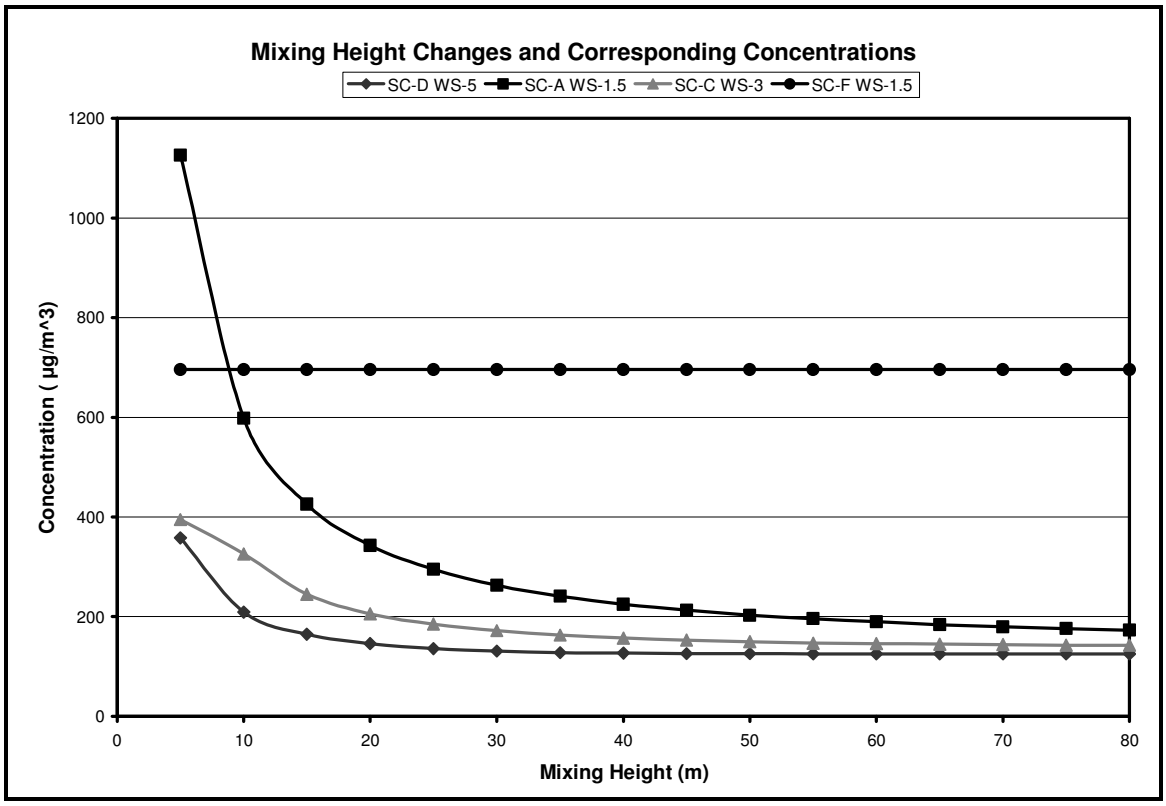

Figure 10. Concentrations produced using ISCST3 corresponding to mixing height changes and various stability classes with average wind speeds. Each stability class is denoted in the legend by the prefix "SC-" and the wind speed is denoted by the prefix "WS-".

The average stability class and wind speed actually measured during the evening dust peak was combined with the theoretical change in mixing height to obtain the contribution that the mixing height could attribute to the changes in concentration measured during the evening dust peak. The change in concentration predicted using ISCST3 remains low until the mixing height of 40 m is reached, where the relationship increases dramatically. A mixing height change from 40 m to 10 m can result in a doubling of the concentration. Figure 9 suggests that a mixing height between 10 and 20 meters would be possible. A mixing height change from 40 to 10 m, coupled with

variations in wind speed and stability class, could account for as much as 70 to 80 percent of the increase in measured evening concentrations.

ROAD AND FEEDLOT CONTRIBUTION ANALYSIS

Because of the rain event the week prior to the April 2004 sampling trip, the feedlot surface's moisture content was increased, thereby reducing the pen surface emissions.

Table 9 represents the ranges in concentrations due to different silt contents used for the road emission flux calculation and a range of stability classes with corresponding wind speeds. The range of silt contents were used to approximate the concentrations that were possible downwind of the feedyard. The range of stability classes was used to approximate concentrations at any time of day or night downwind of the feedyard.

The concentration contribution due to unpaved road emissions was averaged for each of the three road emission fluxes over the range of stability classes and wind speeds. The results indicate that an unpaved road emission flux containing 15% silt will only produce concentrations that are approximately double the concentrations produced from an emission flux with 5% silt content. This suggests a non-linear relationship between silt content and the concentrations produced using the emission fluxes calculated using silt content. Table 9 also suggests that if the pen surface emission factor of 2.7 kg/1000hd-day were used with unpaved road emission fluxes calculated using silt content, approximately 63-75% of the concentrations predicted downwind would be due to unpaved road emissions.

Table 10 lists the results of the analysis utilized to calculate the road emission flux necessary to produce the measured concentrations from certain tests and samplers from the two sampling trips. Despite the four different test sets of measured meteorological conditions and the constant emission rate from the feedyard, the fluxes necessary to produce the N1 ground level concentration are all within an order of magnitude. A weighted average of these four fluxes was 235 $\mu g/m^2$-s.

Table 9. Concentrations predicted using ISCST3 at a receptor located 10 m downwind of the feedyard. The different silt percentages represent different emission fluxes associated with those percentages. The range of stability classes and wind speeds used was to calculate a range of concentrations possible downwind of a feedyard. The wind direction was not allowed to vary in this analysis.

Stability Classes	Wind Speed (m/s)	Concentrations due to the pen surface emissions ($\mu g/m^3$)	Concentrations due to unpaved road emissions (5% silt) ($\mu g/m^3$)	Concentrations due to unpaved road emissions (10% silt) ($\mu g/m^3$)	Concentrations due to unpaved road emissions (15% silt) ($\mu g/m^3$)	Max % due to roads
Day						
A	1.5	26	28	53	76	75
B	2.5	25	22	42	60	71
B	4	16	14	26	38	67
C	5.5	17	13	25	35	67
C	6	16	12	23	32	67
Night						
F	1.5	193	80	150	215	53
E	2.5	81	42	79	114	59
E	4	51	26	50	71	58
D	5.5	28	17	32	45	62
D	6	25	16	29	42	63

Table 10. Unpaved road fluxes necessary to produce average measured concentrations during two test periods for each of the sampling trips. The test periods were chosen because they occurred in the morning when there was road traffic and no abnormal meteorological conditions.

Trip and Test	Average Required Road Flux ($\mu g/m^2$-s)
July 2003	
Test 6	108
Test 15	435
April 2004	
Test 11	119
Test 17	199

This procedure allows the determination of the unpaved road emission rate if the pen surface emission rate is known and vice versa. Because the measured concentration is fixed, a change in either the unpaved road (vehicle traffic) or pen surface (cattle activity) emissions requires a change in the other to maintain the measured concentration. If the pen surface emission rate increases, the road emission must decrease so that the measured concentration is preserved. The opposite is also true. The pen surface emission rate must decrease whenever the unpaved road emissions increase to maintain the measured concentration. This relationship (See Equation 9) between the two sources of fugitive emissions on the feedyard was used to calculate the unpaved road emission rate necessary to maintain a measured concentration given a constant pen surface emission rate.

Wanjura et al. (2004) concluded that up to 80% of the concentrations measured downwind of a feedyard were due to unpaved road emissions (vehicle traffic). The highest percent contribution due to unpaved roads in Table 9 is when the 15% silt emission factor is used with the A stability class and a wind speed of 1.5 m/s. The

percent contribution from the unpaved roads for this point was calculated to be 53%. However, the emission factor for the pen surface reported by Wanjura et al. (2004) was less than half of the emission factor used for the analysis that produced Table 10. Using the relationship developed in the procedure that produced Table 10, (if the pen surface emission rate decreases, then the road emission rate must increase to maintain the measured concentration) it is possible that up to 75% of the concentrations measured downwind of the feedyard may be attributed to unpaved road emissions (vehicle traffic). This suggests that the conclusions formed by Wanjura et al. (2004) are possible.

SCIENCE BASIS FOR ISCST3 AREA SOURCE

The concentration results from modeling a cattle feedyard with unpaved roads using both ISCST3 and the ILSA are compared in Table 11. The concentration results from both models suggest that it is likely that ISCST3 uses a form of the ILSA to calculate concentrations from an area source. The area sources in the schematic of the feedyard (Figure 4) used in ISCST3 were the cattle pens. The results from ISCST3 and ILSA for the pen surface concentrations are almost identical. The concentration results from ILSA for the roads were higher than those predicted using ISCST3. The cause for this lies in the road closest to the receptor. The concentration calculated for this road using ILSA is almost one and a half times that of the concentration calculated using ISCST3.

Table 11. List of PM_{10} concentrations predicted for the cattle feedyard with unpaved roads at 10 meters downwind using ISCST3 and the ILSA.

Emission Source	Concentrations, $\mu g/m^3$, for each model	
	ISCST3	ILSA
Pen Surface	126	126
Unpaved roads	31	45
Total	188	204

The unpaved road closest to the receptor is the source of the discrepancy between ISCST3 and ILSA. By increasing the distance from the edge of the road to the receptor to 30 meters, the concentrations match closely. The concentrations corresponding to a receptor placed 30 meters downwind are shown in Table 12.

Table 12. List of PM_{10} concentrations predicted for the cattle feedyard with unpaved roads at 30 meters downwind using ISCST3 and the ILSA.

Emission Source	Concentrations, $\mu g/m^3$, for each model	
	ISCST3	ILSA
Pen Surface	67	66
Unpaved roads	16	17
Total	83	83

CONCLUSIONS

The following are the findings of this study:

Objective 1. Quantify changes in fugitive particulate matter concentrations downwind of the feedyard based on meteorological conditions and/or cattle activity.

- Up to 40% of the evening concentration increases can be attributed to wind velocity and the corresponding stability class changes
- When the mixing height is reduced from 1000 meters to below 20 meters using ISCST3, the concentrations double.
- The combined effects of decreasing mixing height and changes in wind speed and stability class at the same time period of the evening dust peaks can account for approximately 80% of the concentration increase.
- It is unlikely that cattle activities are the sole source of the evening dust peak
- Meteorological conditions likely influence concentrations downwind, and may play the primary role of the concentration increases during the evening dust peaks. This study did not provide the data necessary to prove or disprove this hypothesis.
- The hypothesis that a combination of cattle activity and meteorological conditions are the primary cause of the evening dust peaks could not be proved or disproved through the results of this research.

Objective 2. Quantify the mass contribution of PM emissions of road dust (vehicle traffic) and pen dust (cattle activity) to the measured concentrations and ultimately PM emission rates of cattle feedyard fugitive sources.

- It is likely that Wanjura et al.'s (2004) report that 80% of the concentrations measured downwind of the feedyard were due to unpaved road emissions (vehicle traffic) is possible for a feedyard.
- Using a ratio, the unpaved road emission rate can be determined if the pen surface emission rate, a downwind concentration, and meteorological conditions are known using ISCST3.

Objective 3. Compare an estimation of concentrations from a feedyard with roads using the infinite line source algorithm with concentrations produced by ISCST3 for the same feedyard setup.

- ISCST3 uses a form of the line source algorithm to estimate the concentrations downwind of an area source.
- At a distance less than 20 meters from the source to the receptor, the infinite line source algorithm concentration predictions do not match ISCST3.

Using the results of this study, the development and use of more effective and efficient strategies to mitigate the emissions from a cattle feedyard is possible. It is possible to predict the occurrence of the evening dust peak, making watering of the pen surface at an appropriate time before sunset extremely effective in reducing dust emissions. With less dust entrained in the air, the effect that meteorological conditions have on changing concentrations during the evening is decreased. The portion of concentrations due to unpaved road emissions can be reduced dramatically by watering the roads. This would decrease a significant portion of the concentration measurements downwind.

RECOMMENDATIONS FOR FUTURE WORK

To better understand the nature of the evening dust peak, equipment such as LIDAR would be valuable for mapping the height and shape of the plume during the evening period. A clearer picture of the particulate matter dispersion during the evening dust peak would allow the application of dispersion models to be more accurate or foster the development of a better dispersion model for cattle feedyards.

Tracking cattle movement during the evening periods would allow a better estimate of how cattle activities contribute to the evening dust peak. Also, it would assist in learning how long the change in cattle activity lasts and if it is related to the start and end of the changes in concentration during the evening dust peak.

Sampling a feedlot for an extended period of time with the roads left dry for the first half of the sampling period and then watered constantly for the second half would assist in developing separate emission factors for the pen surface and unpaved roads. Monitoring of the unpaved road traffic and logging the miles traveled would aid in determining the accuracy of current emission factors for the unpaved roads. The determination of the relationship between moisture content of the unpaved roads and the pen surfaces with the ability to emit particulate matter would help determine the amount of water necessary to reduce emissions.

REFERENCES

Algeo, J. W., C.J. Elam, A. Martinez, and T. Westling. 1972. How to control feedlot pollution: Bulletin D. California Beef Cattle Feeders Association, Bakersfield, CA.

Auvermann, B. W. 2001. Lesson 42: Controlling dust and odor from open-lot livestock facilities. In: *National Animal Manure Management Curriculum*. Ames, IA: Midwest Plan Service.

Clean Air Act (CAA). 1990. The Clean Air Act and subsequent amendments. 42 U.S.C. 7401 et Seq. Washington, DC.

Code of Federal Regulations (CFR). 1986a. Prevention of significant deterioration of air quality. 40 CFR, Chapter 1, Part 51. Office of the Federal Register, National Archives, and Records Administration. Washington DC: U.S. Government Printing Office.

Code of Federal Regulations (CFR). 1986b. Review of new sources and modifications – permit requirements. 40 CFR, Chapter 1, Part 52, Section 165. Office of the Federal Register, National Archives, and Records Administration. Washington DC: U.S. Government Printing Office.

Code of Federal Regulations (CFR). 1996. Federal operating permit program. 40 CFR, Part 71. Office of the Federal Register, National Archives, and Records Administration. Washington DC: U.S. Government Printing Office.

Code of Federal Regulations (CFR). 1999. National primary and secondary ambient air quality standards. 40 CFR, Part 50. Office of the Federal Register, National Archives, and Records Administration. Washington DC: U.S. Government Printing Office.

Code of Federal Regulations (CFR). 2003. Guideline on air quality models. 40 CFR, Chapter 1, Part 51, App. W. Office of the Federal Register, National Archives, and Records Administration. Washington DC: U.S. Government Printing Office.

Cooper, C. D. and F.C. Alley. 2002. *Air Pollution Control: A Design Approach*. 3rd Edition. Prospect Heights, IL: Waveland Press, Inc.

Hamm, L.B., M.D. Buser, S.C. Capareda. J.D. Wanjura, C.B. Parnell Jr., B.W. Shaw. 2005. Cotton gin yard and road dust emissions and the resulting effects on downwind samplers. In *Proceedings of the 2005 Beltwide Cotton Conferences*. Nashville, TN: National Cotton Council.

Holzworth, G. C., 1972. *Mixing heights, wind speeds, and potential for urban air pollution throughout the contiguous United States*. Office of Air Programs AP-10, Environmental Protection Agency, Research Triangle Park, NC.

Mitloehner, F. M., J. L. Morrow-Tesch, J. W. Bailey, and J. J. McGlone. 1999. Altering feeding times for feedlot cattle reduced dust generating behaviors. *J. Anim. Sci.* 77(Suppl 1):148.

Parnell, S., B.J. Lesikar, J.M. Sweeten, B.T. Weinheimer. 1993. Dispersion modeling for prediction of emission factors. Paper No. 934554 presented at the 1993 International Winter Meeting sponsored by the American Society of Agricultural Engineers, Chicago, IL. American Society of Agricultural Engineers, St. Joseph, MI.

Parnell, C.B., B.W. Shaw, B.W. Auvermann. 1999. Agricultural air quality fine particle project: task 1 livestock – feedlot particulate matter emission factors and emission inventory estimates. Texas Natural Resource Conservation Commission. Austin, TX.

Peters, J.A., T.R. Blackwood. 1977. Source assessment: beef cattle feedlots. EPA-600/2-77-107. Monsanto Research Corporation, Dayton, OH for EPA Office of Research and Development, Industrial Environmental Research Laboratory, Research Triangle Park, NC.

Rupprecht & Pataschnick Co., Inc. 2002. *Operating manual – TEOM Series 1400a Ambient Particulate (PM-10) Monitor.* Revision B. Albany, NY: Rupprecht & Pataschnick Co., Inc.

Sweeten, J.M., C.B. Parnell, R.S. Etheredge, D. Osborne. 1988. Dust emissions in cattle feedlots. In: *Veterinary Clinics of North America: Food Animal Practice*; Vol. 4, No. 3. Philidelphia, PA: W.B. Saunders.

Sweeten, J.M., C.B. Parnell, B.W. Shaw, B.W. Auvermann. 1998. Particle size distribution of cattle feedlot dust emission. *Trans. ASAE* 41(5): 1477-1481.

Trinity Consultants. 2000. Practical guide to atmospheric dispersion modeling. Computer modeling short course reference material. Dallas, TX: Trinity Consultants.

Trinity Consultants. 2002. *Breeze ISC GIS-Pro*. Ver. 4.0.13. Dallas, TX: Trinity Consultants.

Turner, D. B. 1994. *Workbook of Atmospheric Dispersion Estimates – An Introduction to Dispersion Modeling* (Second Edition). Boca Raton, FL: Lewis Publishers; CRC Press, Inc.

U.S. Environmental Protection Agency (USEPA). 1985. *Compilation of Air Pollutant Emission Factors*, 4th Edition. Vol.1 - Stationary Point and Area Sources. Research Triangle Park, NC: USEPA, Office of Air Quality Planning and Standards, Emission Factors and Inventory Group.

U.S. Environmental Protection Agency (USEPA). 1995. *Compilation of Air Pollutant Emission Factors*, 5th Edition. Research Triangle Park, NC: USEPA, Office of Air Quality Planning and Standards, Emission Factors and Inventory Group.

U.S. Environmental Protection Agency (USEPA). 2000. *Meteorological Monitoring Guidelines for Regulatory Modeling Applications.* EPA-454/R-99-005. Research Triangle Park, NC: US Environmental Protection Agency, Office of Air Quality Planning and Standards Emission Factors and Inventory Group.

U.S. Naval Observatory (USNO). 2005. Complete sun and moon data for one day. Astronomical Applications Department. Available at http://aa.usno.navy.mil/. Accessed May 11, 2005.

Wang, L., J.D. Wanjura, C. Boriack, C.B. Parnell, Jr., B.W. Shaw, and R.E. Lacey. 2003. Performance characteristics of low-volume PM10 inlet and TEOM continuous PM sampler. Presented at the 2003 Annual International Meeting of the ASAE held from July 27-30, 2003 at Las Vegas, NV. Paper No. 034118.

Wanjura, J. D., C. B. Parnell, B. W. Shaw and R. E. Lacey. 2003. Design and evaluation of a low volume total suspended particulate sampler. In *Proceedings of the 2003 Beltwide Cotton Conferences*, National Cotton Council, Nashville, TN.

Wanjura, J.D., C.B. Parnell, B.W. Shaw, R.E Lacey. 2004. A protocol for determining a fugitive dust emission factor from a ground level area source. Paper No.044018. Presented at the 2004 Annual International Meeting of the American Society of Agricultural Engineers and Canadian Society of Agricultural Engineers, Ottowa, Ontario, Canada.

Wark, K., C.E. Warner, W.T. Davis. 1998. *Air Pollution Its Origin and Control.* 3rd Edition. Menlo Park, CA: Addison Wesley Longman, Inc.

APPENDIX A

CONCENTRATION DATA MEASURED AND CALCULATED FOR JULY 2003 AND APRIL 2004

Table A-1. Concentration Data sorted by test and sampler location for the July 2003 sampling trip. An S, E, W, N1, or N2 at the beginning of the sampler name denotes the location of the sampler, with a T indicating the 10 m tower at the North 1 location. LV denotes low volume sampler, with PM10 representing a PM_{10} sampler and TSP a total suspended particulate sampler.

Test Number	Sampler	Concentration ($\mu g/m^3$)
2	ELVPM10	498
2	ELVTSP	921
2	N1LVPM10	4925
2	N1LVTSP	576
2	N2LVPM10	1484
2	N2LVTSP	1642
2	SLVPM10	107
2	SLVTSP	94
2	T7	1563
2	T9	1037
2	WLVTSP	63
5	ELVPM10	1594
5	ELVTSP	2535
5	N1LVPM10	609
5	N1LVTSP	612
5	N2LVPM10	649
5	N2LVTSP	1091
5	SLVPM10	533
5	SLVTSP	108
5	T5	804
5	T7	622
5	T9	423
5	WLVTSP	147
6	ELVPM10	631
6	ELVTSP	1003
6	N1LVPM10	562
6	N1LVTSP	728
6	N2LVPM10	537
6	N2LVTSP	1097
6	SLVPM10	358
6	SLVTSP	151
6	T5	1165
6	T7	997
6	T9	667
6	WLVTSP	104
7	ELVPM10	1172
7	ELVTSP	1796
7	N1LVPM10	74
7	N1LVTSP	432
7	N2LVPM10	9195
7	N2LVTSP	1081
7	SLVPM10	528
7	SLVTSP	66

Table A-1 Continued

Test Number	Sampler	Concentration ($\mu g/m^3$)
7	T5	694
7	T7	700
7	T9	697
7	WLVPM10	145
7	WLVTSP	242
8	ELVPM10	648
8	ELVTSP	1019
8	N1LVPM10	402
8	N1LVTSP	355
8	N2LVPM10	350
8	N2LVTSP	515
8	SLVPM10	93
8	SLVTSP	67
8	T7	707
8	T9	392
8	WLVPM10	140
8	WLVTSP	129
9	ELVPM10	315
9	ELVTSP	0
9	N1LVPM10	154
9	N1LVTSP	194
9	N2LVPM10	346
9	N2LVTSP	523
9	SLVPM10	71
9	SLVTSP	82
9	T7	376
9	T9	326
9	WLVPM10	259
9	WLVTSP	204
10	ELVPM10	175
10	ELVTSP	209
10	N1LVPM10	3414
10	N1LVTSP	2499
10	N2LVPM10	6806
10	N2LVTSP	10223
10	SLVPM10	187
10	SLVTSP	133
10	T7	5425
10	T9	2887
10	WLVPM10	6891
10	WLVTSP	6290
11	ELVPM10	95
11	ELVTSP	78
11	N1LVPM10	803

Table A-1 Continued

Test Number	Sampler	Concentration ($\mu g/m^3$)
11	N1LVTSP	695
11	N2LVPM10	1523
11	N2LVTSP	2274
11	SLVPM10	205
11	SLVTSP	23
11	T7	1430
11	T9	915
11	WLVPM10	1465
11	WLVTSP	1566
12	ELVPM10	505
12	ELVTSP	807
12	N1LVPM10	545
12	N1LVTSP	654
12	N2LVPM10	689
12	N2LVTSP	1166
12	SLVPM10	247
12	SLVTSP	62
12	T5	975
12	T7	1043
12	T9	800
12	WLVPM10	418
13	ELVPM10	503
13	ELVTSP	1025
13	N1LVPM10	367
13	N1LVTSP	417
13	N2LVPM10	270
13	N2LVTSP	553
13	SLVPM10	229
13	SLVTSP	251
13	T5	674
13	T7	747
13	T9	511
13	WLVPM10	162
13	WLVTSP	107
14	ELVPM10	650
14	ELVTSP	1022
14	N1LVPM10	565
14	N2LVPM10	750
14	N2LVTSP	1134
14	SLVPM10	99
14	SLVTSP	135
14	T5	888
14	T7	1241
14	T9	743
14	WLVPM10	796

Table A-1 Continued

Test Number	Sampler	Concentration ($\mu g/m^3$)
14	WLVTSP	465
15	ELVPM10	112
15	ELVTSP	94
15	N1LVPM10	566
15	N2LVPM10	851
15	N2LVTSP	1110
15	SLVPM10	66
15	SLVTSP	56
15	T5	1098
15	T7	851
15	T9	955
15	WLVPM10	1110
15	WLVTSP	1340
16	ELVPM10	112
16	ELVTSP	96
16	N1LVPM10	727
16	N2LVPM10	960
16	N2LVTSP	1409
16	SLVPM10	135
16	SLVTSP	105
16	T5	1018
16	T7	1059
16	T9	848
16	WLVPM10	1283
16	WLVTSP	1395
17	ELVPM10	152
17	ELVTSP	145
17	N1LVPM10	3009
17	N2LVPM10	5170
17	N2LVTSP	11231
17	SLVPM10	82
17	SLVTSP	65
17	T5	6830
17	T7	5302
17	T9	3121
17	WLVPM10	4761
17	WLVTSP	8072
18	ELVPM10	205
18	ELVTSP	387
18	N1LVPM10	395
18	N2LVPM10	683
18	N2LVTSP	1308
18	SLVPM10	92
18	SLVTSP	51
18	T5	730

Table A-1 Continued

Test Number	Sampler	Concentration (µg/m^3)
18	T7	944
18	T9	604
18	WLVPM10	849
18	WLVTSP	1242
19	ELVPM10	571
19	ELVTSP	1186
19	N1LVPM10	293
19	N1LVTSP	458
19	N2LVPM10	196
19	N2LVTSP	539
19	SLVPM10	1226
19	SLVTSP	95
19	T5	686
19	T7	705
19	T9	0
19	WLVPM10	3221
19	WLVTSP	56
20	ELVPM10	606
20	ELVTSP	853
20	N1LVPM10	321
20	N1LVTSP	328
20	N2LVPM10	354
20	N2LVTSP	838
20	SLVPM10	26
20	SLVTSP	43
20	T5	766
20	T7	891
20	T9	674
20	WLVPM10	56
20	WLVTSP	90
21	ELVPM10	390
21	ELVTSP	566
21	N1LVPM10	327
21	N1LVTSP	436
21	N2LVPM10	560
21	N2LVTSP	1173
21	SLVPM10	59
21	SLVTSP	53
21	T5	787
21	T7	748
21	T9	495
21	WLVPM10	194
21	WLVTSP	302

Table A-2. Concentration Data sorted by test and sampler location for the April 2004 sampling trip. An S, E, W, N1 or N2 at the beginning of the sampler name denotes the sampler location, with a T indicating the 10 m tower at the North 1 location. LV denotes low volume, with PM10 representing a PM_{10} sampler and TSP representing a total suspended particulate sampler.

Test Number	Sampler	Concentration ($\mu g/m^3$)
1	SLVPM10	73
1	SLVTSP	36
1	ELVPM10	369
1	ELVTSP	719
1	N1LVPM10	158
1	N1LVTSP	172
1	T5	136
1	T7	75
1	N2LVTSP	149
1	N2LVPM10	321
1	WLVTSP	368
1	WLVPM10	53
1	T9	72
2	SLVPM10	21
2	SLVTSP	47
2	ELVPM10	232
2	ELVTSP	681
2	N1LVPM10	553
2	N1LVTSP	857
2	T5	422
2	T7	304
2	N2LVTSP	591
2	N2LVPM10	402
2	WLVTSP	32
2	WLVPM10	69
2	T9	362
3	SLVPM10	110
3	SLVTSP	60
3	ELVPM10	176
3	ELVTSP	252
3	N1LVPM10	110
3	N1LVTSP	267
3	T5	117
3	T7	158
3	N2LVTSP	152
3	N2LVPM10	117
3	WLVTSP	60
3	WLVPM10	52
3	T9	87
4	SLVPM10	20
4	SLVTSP	43
4	ELVPM10	160
4	ELVTSP	408

Table A-2 Continued

Test Number	Sampler	Concentration (µg/m^3)
4	N1LVPM10	50
4	N1LVTSP	108
4	T5	69
4	T7	59
4	N2LVTSP	69
4	N2LVPM10	53
4	WLVTSP	32
4	WLVPM10	22
4	T9	44
5	SLVPM10	66
5	SLVTSP	79
5	ELVPM10	790
5	ELVTSP	1456
5	N1LVPM10	92
5	N1LVTSP	123
5	T5	92
5	T7	132
5	N2LVTSP	55
5	N2LVPM10	155
5	WLVTSP	68
5	WLVPM10	37
5	T9	89
6	SLVPM10	64
6	SLVTSP	134
6	ELVPM10	2196
6	ELVTSP	1799
6	N1LVPM10	157
6	N1LVTSP	162
6	T5	142
6	T7	65
6	N2LVTSP	149
6	N2LVPM10	181
6	WLVTSP	24
6	WLVPM10	44
6	T9	62
7	SLVPM10	49
7	SLVTSP	81
7	ELVPM10	720
7	ELVTSP	1517
7	N1LVPM10	199
7	N1LVTSP	299
7	T5	153
7	T7	334
7	N2LVTSP	226
7	N2LVPM10	266

Table A-2 Continued

Test Number	Sampler	Concentration (µg/m^3)
7	WLVTSP	50
7	WLVPM10	30
7	T9	173
8	SLVPM10	162
8	SLVTSP	946
8	ELVPM10	0
8	ELVTSP	1038
8	N1LVPM10	1188
8	N1LVTSP	1840
8	T5	1558
8	WLVTSP	113
8	WLVPM10	0
8	T9	0
9	SLVPM10	17
9	SLVTSP	57
9	ELVPM10	0
9	ELVTSP	297
9	N1LVPM10	300
9	N1LVTSP	565
9	T5	337
9	T7	255
9	N2LVTSP	348
9	N2LVPM10	215
9	WLVTSP	311
9	WLVPM10	0
9	T9	210
10	SLVPM10	39
10	SLVTSP	27
10	ELVPM10	99
10	ELVTSP	38
10	N1LVPM10	52
10	N1LVTSP	39
10	T5	83
10	T7	55
10	N2LVTSP	83
10	N2LVPM10	79
10	WLVTSP	0
10	WLVPM10	76
10	T9	80
11	SLVPM10	65
11	SLVTSP	95
11	ELVPM10	1017
11	ELVTSP	1232
11	N1LVPM10	42
11	N1LVTSP	358

Table A-2 Continued

Test Number	Sampler	Concentration (µg/m^3)
11	T5	109
11	T7	41
11	N2LVTSP	159
11	N2LVPM10	139
11	WLVTSP	118
11	T9	330
12	SLVPM10	68
12	SLVTSP	0
12	ELVTSP	795
12	N1LVPM10	169
12	N1LVTSP	333
12	T5	278
12	T7	100
12	N2LVTSP	265
12	N2LVPM10	143
12	WLVTSP	135
12	WLVPM10	73
12	T9	128
13	SLVPM10	1
13	SLVTSP	83
13	ELVPM10	292
13	ELVTSP	532
13	N1LVPM10	198
13	N1LVTSP	233
13	T5	257
13	T7	165
13	N2LVTSP	234
13	N2LVPM10	160
13	WLVTSP	65
13	WLVPM10	55
13	T9	246
14	SLVPM10	62
14	SLVTSP	73
14	ELVPM10	4943
14	ELVTSP	629
14	N1LVPM10	494
14	N1LVTSP	989
14	T5	764
14	T7	583
14	N2LVTSP	798
14	N2LVPM10	403
14	WLVTSP	1063
14	WLVPM10	582
14	T9	487
15	SLVPM10	38

Table A-2 Continued

Test Number	Sampler	Concentration (µg/m^3)
15	SLVTSP	33
15	ELVPM10	126
15	ELVTSP	390
15	N1LVTSP	298
15	T5	190
15	T7	132
15	N2LVTSP	208
15	N2LVPM10	104
15	WLVTSP	76
15	WLVPM10	68
15	T9	173
16	SLVPM10	18
16	SLVTSP	77
16	ELVPM10	75
16	ELVTSP	89
16	N1LVPM10	52
16	N1LVTSP	75
16	T5	88
16	T7	37
16	N2LVTSP	73
16	N2LVPM10	36
16	WLVTSP	52
16	WLVPM10	3
16	T9	79
17	SLVPM10	90
17	SLVTSP	149
17	ELVPM10	681
17	ELVTSP	1552
17	N1LVPM10	146
17	N1LVTSP	437
17	T5	513
17	T7	297
17	N2LVTSP	336
17	N2LVPM10	176
17	WLVTSP	217
17	WLVPM10	40
17	T9	297
18	SLVPM10	132
18	SLVTSP	75
18	ELVPM10	740
18	ELVTSP	1629
18	N1LVPM10	1222
18	N1LVTSP	434
18	T5	685
18	T7	336

Table A-2 Continued

Test Number	Sampler	Concentration (µg/m^3)
18	N2LVTSP	606
18	WLVTSP	157
18	T9	414
19	SLVPM10	26
19	SLVTSP	33
19	ELVPM10	348
19	N1LVPM10	264
19	N1LVTSP	298
19	T5	324
19	T7	265
19	N2LVTSP	306
19	N2LVPM10	230
19	WLVTSP	306
19	WLVPM10	78
19	T9	206
20	SLVPM10	29
20	SLVTSP	149
20	ELVPM10	313
20	ELVTSP	600
20	N1LVPM10	549
20	N1LVTSP	945
20	T5	647
20	T7	548
20	N2LVTSP	789
20	N2LVPM10	504
20	WLVTSP	41
20	WLVPM10	71
20	T9	441
21	SLVPM10	18
21	SLVTSP	81
21	ELVPM10	230
21	ELVTSP	383
21	N1LVPM10	136
21	N1LVTSP	373
21	T5	213
21	T7	231
21	N2LVTSP	222
21	N2LVPM10	78
21	WLVTSP	123
21	T9	216
22	SLVPM10	20
22	SLVTSP	47
22	ELVPM10	67
22	ELVTSP	120
22	N1LVPM10	36

Table A-2 Continued

Test Number	Sampler	Concentration (µg/m^3)
22	N1LVTSP	86
22	T5	79
22	T7	55
22	N2LVTSP	79
22	N2LVPM10	52
22	WLVTSP	34
22	WLVPM10	31
22	T9	45
23	SLVPM10	86
23	SLVTSP	189
23	ELVPM10	548
23	ELVTSP	1188
23	N1LVPM10	104
23	N1LVTSP	102
23	T5	157
23	T7	86
23	N2LVTSP	278
23	N2LVPM10	93
23	WLVTSP	140
23	WLVPM10	68
23	T9	188
24	SLVPM10	19
24	SLVTSP	102
24	ELVPM10	346
24	ELVTSP	757
24	N1LVPM10	202
24	N1LVTSP	389
24	T5	289
24	T7	182
24	N2LVTSP	456
24	N2LVPM10	201
24	WLVTSP	324
24	WLVPM10	589
24	T9	226

APPENDIX B

PARTICLE SIZE DISTRIBUTION ANALYSIS

A particle size distribution (PSD) analysis was performed on the Total Suspended Particulate (TSP) filters from one of the downwind sampling locations using a Coulter counter (Multisizer 3 Coulter Counter, Beckman Coulter, Inc., Fullerton, CA.). The Coulter counter reports the particle size distribution on an equivalent spherical diameter basis. This is corrected to an aerodynamic equivalent diameter basis using equation B-1. This correction is necessary because current regulation of particulate matter is based on aerodynamic equivalent diameter.

$$AED = ESD \times \sqrt{\rho_{particle}} \qquad \text{(B-1)}$$

where AED = aerodynamic equivalent diameter, μm;

ESD = equivalent spherical diameter (what the Coulter Counter produces), μm; and

$\rho_{particle}$ = particle density of the particulate matter being analyzed, g/cm^3.

The value used for the particle density in this research was 2.33 g/cm^3. This was determined by taking a sample of feedyard dust and using a pycnometer (AccuPyc 1330 Pycnometer, Micromeritics Instrument Corp., Norcross, GA) to determine the particle density.

The particle size distribution can best be characterized using a log-normal distribution with two parameters: mass median diameter (MMD) and geometric standard deviation (GSD). The GSD for this distribution can be found by equation B-2.

$$GSD = \frac{d_{84.1}}{d_{50}} = \frac{d_{50}}{d_{15.9}} \qquad \text{(B-2)}$$

where GSD = geometric standard deviation;

$d_{84.1}$ = particle diameter that 84.1% of the mass of particles is less than in diameter, μm;

d_{50} = particle diameter that 50% of the mass of particles is less than in diameter, μm;

$d_{15.9}$ = particle diameter that 15.9% of the mass of particles is less than in diameter, μm.

Because the particle size distribution does not exactly match the log-normal distribution, an average of the two GSD ratios in equation B-2 is calculated as the GSD. The MMD (ESD) of a particle size distribution is equivalent to the d_{50} reported by the Coulter counter. The approximation of the PSD represented by the log-normal distribution can be used to calculate the mass percentage of certain size particles such as PM_{10} and $PM_{2.5}$ from the TSP concentration.

Table B-1 lists the MMD, GSD, and PM_{10} % calculated using the Coulter counter from the North 1 location during the July 2003 sampling trip. PSDs were calculated from the tower TSP samplers as well as the ground level sampler. The PSDs for the April 2004 sampling trip were described by Wanjura et al. (2004).

Table B-1. List of mass median diameters, geometric standard deviations, and the percentage of PM_{10} for each of the TSP samplers at the North 1 location during the July 2003 sampling trip. Sampler designations with "T" and a number represent the tower and the height on the tower at which the sampler was located.

Sampler	Test	MMD	GSD	% PM10
T7	1	16.9	2.5	28%
T5	2	17.3	2.2	25%
T7	2	21.2	2.4	20%
N1LVTSP	4	12.3	2.0	38%
T5	4	13.8	2.0	33%
T7	4	11.7	2.1	42%
T9	4	12.4	2.2	39%
N1LVTSP	5	15.3	2.1	28%
T5	5	15.3	2.1	28%
T9	5	16.4	2.1	26%
N1LVTSP	6	15.3	1.9	26%
T5	6	19.0	1.9	16%
T7	6	18.6	2.0	19%
T9	6	15.3	2.0	27%
N1LVTSP	7	15.1	2.1	29%
N1LVTSP	8	15.9	2.4	30%
N1LVTSP	9	15.6	2.2	28%
T5	9	18.3	2.2	22%
T7	9	16.7	2.1	25%
T9	9	17.2	2.3	25%
N1LVTSP	10	14.1	2.0	31%
T5	10	13.9	2.0	31%
T7	10	14.1	2.0	31%
N1LVTSP	11	12.8	1.9	35%
T5	11	13.6	2.0	33%
T7	11	14.3	2.0	31%
T9	11	15.5	2.1	28%
T5	12	14.2	2.1	32%
T7	12	14.4	2.0	30%
T9	12	15.5	2.1	28%
T5	13	15.0	2.0	28%
T7	13	15.7	2.0	25%
T9	13	14.0	2.2	33%
N1LVTSP	14	13.9	2.2	34%
T5	14	20.3	2.0	16%
T7	14	15.0	2.1	29%
T9	14	18.8	2.1	20%
T5	15	19.7	2.3	20%
T7	15	16.7	2.3	26%
T9	15	23.2	2.3	15%
N1LVTSP	16	23.0	2.3	15%
T5	16	21.4	2.3	18%
T7	16	22.4	2.2	15%

Table B-1 Continued

Sampler	Test	MMD	GSD	% PM10
T9	16	26.5	1.9	7%
N1LVTSP	17	11.6	2.0	42%
T5	17	16.7	2.2	25%
T7	17	18.0	2.3	24%
T9	17	17.7	2.3	24%
N1LVTSP	18	16.7	2.0	22%
T5	18	16.0	1.9	24%
T7	18	16.6	2.0	23%
T9	18	17.5	1.9	19%
N1LVTSP	19	16.3	1.9	23%
T5	19	15.8	2.0	26%
T7	19	16.3	2.0	24%
T9	19	16.1	2.0	25%
N1LVTSP	20	18.2	2.2	22%
N1LVTSP	21	24.0	2.3	14%
T5	21	28.3	2.1	8%

The average PSD for each of the samplers is shown in Table B-2.

Table B-2 - Average particle size distribution for each of the samplers at the North 1 location measured during the July 2003 sampling trip.

Sampler	average MMD	Average GSD	Average % PM10
N1LVTSP	16.0	2.10	28.2%
T5	17.4	2.08	24.0%
T7	16.6	2.13	26.1%
T9	17.4	2.11	24.4%

APPENDIX C

EXAMPLE OF ISCST3 METEOROLOGICAL DATA INPUT

Table C-1. Example set of meteorological data that could be used as input into ISCST3. The numbers in the stability class column represent the 6 stability classes based on Turner (1994), with 1=A, 2=B, etc. The flow vector is the direction toward which the wind is blowing.

Year	Month	Day	Hour	Flow Vector	Wind Speed (m/s)	Temperature (K)	Stability Class	Rural Mixing Height (m)	Urban Mixing Height (m)
01	01	01	01	360	1.5	298	1	1000	1000
01	01	01	02	360	2.5	298	2	1000	1000
01	01	01	03	360	6	298	3	1000	1000
01	01	01	04	360	6	298	4	1000	1000
01	01	01	05	360	2.5	298	5	1000	1000
01	01	01	06	360	1.5	298	6	1000	1000
01	01	01	07	360	1.5	298	1	80	80
01	01	01	08	360	2.5	298	2	80	80
01	01	01	09	360	6	298	3	80	80
01	01	01	10	360	6	298	4	80	80
01	01	01	11	360	2.5	298	5	80	80
01	01	01	12	360	1.5	298	6	80	80
01	01	01	13	360	1.5	298	1	20	20
01	01	01	14	360	2.5	298	2	20	20
01	01	01	15	360	6	298	3	20	20
01	01	01	16	360	6	298	4	20	20
01	01	01	17	360	2.5	298	5	20	20
01	01	01	18	360	1.5	298	6	20	20
01	01	01	19	360	1.5	298	1	5	5
01	01	01	20	360	2.5	298	2	5	5
01	01	01	21	360	6	298	3	5	5
01	01	01	22	360	6	298	4	5	5
01	01	01	23	360	2.5	298	5	5	5
01	01	01	24	360	1.5	298	6	5	5

APPENDIX D

EXAMPLE CALCULATION OF AP-42 EMISSION FACTORS AND CONVERSION INTO AREA SOURCE EMISSION RATES

The AP-42 emission factor is calculated using equation D-1.

$$EF = k(s/12)^a (W/3)^b \quad \text{(D-1)}$$

where EF = size specific emission factor, lbs/vehicle-mi traveled,

s = surface material silt content, percentage;

W = mean vehicle weight, tons; and

k, a, and b are empirical constants, determined by the emission factor's particulate matter size. Values for the PM_{10} emission factor are k = 1.5, a = 0.9, and b= 0.45.

An example silt content used in this research was 10 %, along with an assumed feed truck weight of 20 tons. Inserting these numbers into the equation D-1, the resulting equation is shown in equation D-2.

$$EF = 1.5(10/12)^{0.9} (20/3)^{0.45} = 2.98 lbs/VMT \quad \text{(D-2)}$$

The result of equation D-2 was used in equation D-3 to determine an area flux for the roads needed in ISCST3.

$$Area\ Flux = \frac{EF \times VMT_{total} \times 454}{L \times W \times t_{truck}} \quad \text{(D-3)}$$

where Area Flux = amount of PM_{10} the truck produces per unit area, g/m^2-s;

EF = AP-42 emission factor for unpaved roads, lbs/VMT;

VMT_{total} = total vehicle miles traveled, miles;

L = length of road that the trucks travel, m;

W = width of the roads, m;

t_{truck} = time necessary for a vehicle to travel the distance, seconds; and

454 is the factor to convert pounds to grams.

To determine the time necessary for the truck to travel the distance, equation D-4 was used.

$$t_{truck} = \frac{VMT_{total}}{S} \times 3600 \qquad \text{(D-4)}$$

where t_{truck} = time it takes for a truck to travel its path, seconds;

S = speed of the truck, mph;

3600 = factor to convert hours to seconds; and

VMT_{total} = vehicle miles traveled by a truck.

The time it takes a truck traveling at 5 mph to travel the length of one of the side roads that has a length of 1134 meters (0.705 miles) is calculated in equation D-5.

$$t_{truck} = \frac{0.705}{5} \times 3600 = 507s \qquad \text{(D-5)}$$

Taking the results of both equation D-5 and D-2 and inserting them into equation D-3 forms the equation shown in D-6.

$$Area\ Flux = \frac{2.98 \times 0.705 \times 454}{1134 \times 10 \times 507} = 166 \mu g / m^2 - s \qquad \text{(D-6)}$$

This is an example of the process used to calculate an area flux emission rate for an ISCST3 line source using the AP-42 unpaved road emission factor.

APPENDIX E

EXAMPLE CALCULATION OF INFINITE LINE SOURCE ALGORITHM AND CONVERSION OF AREA SOURCE EMISSION FLUX TO LINE SOURCE EMISSION RATE

The equation used to determine concentrations using the infinite line source algorithm is shown in equation E-1.

$$C = \frac{2Q_L 10^6}{\sqrt{2\pi}(\sigma_z u)} e^{\left(-\frac{1}{2}\left(\frac{H}{\sigma_z}\right)^2\right)} \quad \text{(E-1)}$$

where C = concentration at some distance downwind, $\mu g/m^3$;

Q_L = line emission rate, g/m;

σ_z = vertical dispersion parameter, meters;

u = wind speed, meters per second; and

H = effective emission height, meters.

The σ_z component was calculated for the above equation by using Equation 12.

$$\sigma_z = aX^b \quad \text{(E-2)}$$

where X = downwind distance to the sampler, kilometers; and

a and b are constants that are dependent upon stability class (Turner, 1994).

The stability class used for this example was "D". The coefficients for stability class "D" are a = 34.5 and b = 0.870. Using a distance of 35 meters (0.03 km, which is required for the equation), the equation results as follows:

$$\sigma_z = (34.5)(0.035)^{0.870} = 1.867\, meters \quad \text{(E-3)}$$

To convert an area source emission flux to a line source emission rate, equation E-4 was used.

$$Q_L = \frac{Q_A * A_{line}}{W_{line}} \quad \text{(E-4)}$$

where Q_A = area emission flux, $\mu g/m^2$-s;

A_{line} = area of the line, m^2; and

W_{line} = width of the line, m;

The width of the line for this analysis was assumed to be 835 m. The area emission flux was the 5% silt content emission factor, 9.5 μg/m^2-s. Using equation E-4, the resulting equation with the numbers inserted is shown in Equation E-5.

$$Q_L = \frac{9.5 \times (10 \times 835)}{835} = 95 \mu g / m - s \qquad \text{(E-5)}$$

The emission height of the cattle is assumed to be zero, given that the dust emissions originate from where the interaction of the hooves and manure pack meet. This sets the effective emission height at 0 m. Using the above determined numbers, equation E-1 becomes equation E-6.

$$C = \frac{2(95 \times 10^{-6})10^6}{\sqrt{2\pi}(1.876)(3)} e^{\left(-\frac{1}{2}\left(\frac{0}{1.876}\right)^2\right)} = 13.5 \mu g / m^3 \qquad \text{(E-6)}$$

VITA

Lee Bradford Hamm received his Bachelor of Science degree in agricultural engineering from Texas A&M University in May, 2003. He entered the Master of Science program in agricultural engineering in August of 2003. His research interests include dust emissions on cattle feed yards. He plans to get a job in engineering consulting and continue from there.

Mr. Hamm may be reached at the Agricultural Engineering Department, attn: Lee Hamm, 201 Scoates Hall, Mail Stop 2117, College Station, Texas, 77840.